Accepted Manuscript

Positional isomers of bispyridine benzene derivatives induce efficacy changes on $mGlu_5$ negative allosteric modulation

Xavier Gómez-Santacana, James A.R. Dalton, Xavier Rovira, Jean Philippe Pin, Cyril Goudet, Pau Gorostiza, Jesús Giraldo, Amadeu Llebaria

PII: S0223-5234(17)30021-1

DOI: 10.1016/j.ejmech.2017.01.013

Reference: EJMECH 9164

To appear in: *European Journal of Medicinal Chemistry*

Received Date: 10 November 2016

Revised Date: 6 January 2017

Accepted Date: 9 January 2017

Please cite this article as: X. Gómez-Santacana, J.A.R. Dalton, X. Rovira, J.P. Pin, C. Goudet, P. Gorostiza, J. Giraldo, A. Llebaria, Positional isomers of bispyridine benzene derivatives induce efficacy changes on $mGlu_5$ negative allosteric modulation, *European Journal of Medicinal Chemistry* (2017), doi: 10.1016/j.ejmech.2017.01.013.

This is a PDF file of an unedited manuscript that has been accepted for publication. As a service to our customers we are providing this early version of the manuscript. The manuscript will undergo copyediting, typesetting, and review of the resulting proof before it is published in its final form. Please note that during the production process errors may be discovered which could affect the content, and all legal disclaimers that apply to the journal pertain.

Positional isomers of bispyridine benzene derivatives induce efficacy changes on $mGlu_5$ negative allosteric modulation

Xavier Gómez-Santacana[a,b,c,§], James A.R. Dalton[b,d], Xavier Rovira[e,f], Jean Philippe Pin[e,f], Cyril Goudet[e,f], Pau Gorostiza[c,g,h], Jesús Giraldo[b,d] and Amadeu Llebaria[a*]

(a) MCS, Laboratory of Medicinal Chemistry & Synthesis, Institute for Advanced Chemistry of Catalonia (IQAC−CSIC), Jordi Girona 18-26, 08034 Barcelona, Spain. (b) Laboratory of Molecular Neuropharmacology and Bioinformatics, Institut de Neurociències and Unitat de Bioestadística, Universitat Autònoma de Barcelona (UAB), 08193 Bellaterra, Spain. (c) Nanoprobes and Nanoswitches, Institute for Bioengineering of Catalonia (IBEC), Baldiri Reixac, 08028, Barcelona, Spain. (d) Network Biomedical Research Center on Mental Health (CIBERSAM), Spain (e) Department of Neurosciences, Institute of Functional Genomics, Université de Montpellier, Unité Mixte de Recherche 5302 CNRS, Montpellier, France; (f) Unité de recherche U1191, INSERM, Montpellier, France (g) Network Biomedical Research Center on Bioengineering, Biomaterials and Nanomedicine (CIBER-BBN), Spain. (h) Catalan Institution for Research and Advanced Studies (ICREA), Barcelona, Spain. (§) Present address: Division of Medicinal Chemistry, Amsterdam Institute for Molecules, Medicines and Systems (AIMMS), VU University Amsterdam, The Netherlands. * Corresponding author: amadeu.llebaria@iqac.csic.es

Keywords: $mGlu_5$, isomers, partial efficacy, NAM, antagonist, inverse agonist

Graphical Abstract

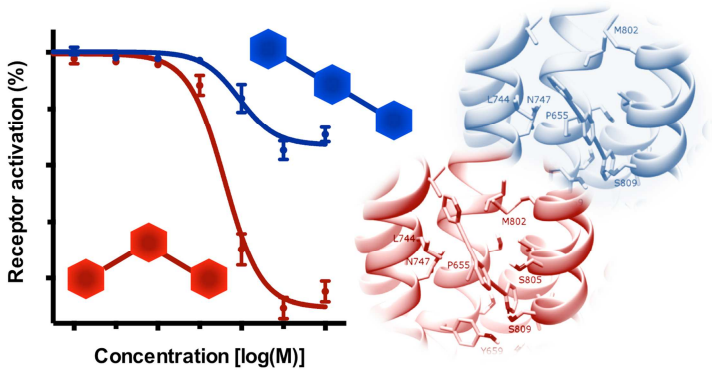

Highlights

- Efficacy of bispyridine benzene mGlu5 negative allosteric modulators depends on molecule geometry.
- 1,4-disubstituted linear compounds have $mGlu_5$ partial antagonist activity.
- 1,3-disubstituted angular compounds have $mGlu_5$ full inverse agonist activity.
- 1,4- and 1,3-isomers bind preferentially to different receptor conformations according to computational docking.

Abstract

Modulation of metabotropic glutamate receptor 5 ($mGlu_5$) with partial allosteric antagonists has received increased interest due to their favourable *in vivo* activity profiles compared to the unfavourable side-effects of full inverse agonists. Here we report on a series of bispyridine benzene derivatives with a functional molecular switch affecting antagonistic efficacy, shifting from inverse agonism to partial antagonism with only a single change in the substitution pattern of the benzene ring. These efficacy changes are explained through computational docking, revealing two different receptor conformations of different energetic stability and different positional isomer binding preferences.

Introduction

Metabotropic glutamate receptors (mGluRs) are class C G Protein-Coupled Receptors (GPCRs) activated by glutamate, the major excitatory neurotransmitter in the central nervous system (CNS). They are widely distributed throughout the CNS, regulating several neuronal and glial functions [1], and are considered potential targets for the treatment of several neurological disorders [2]. The mGlu receptor family comprises eight subtypes classified in three groups based upon sequence homology and molecular function [3]. In particular, subtype 5 ($mGlu_5$) belongs to group I mGluRs and is mainly postsynaptic. Current research indicates that inactivating $mGlu_5$ may be an effective treatment for neuropathic and inflammatory pain [4, 5] and may exert a neuroprotective effect on dopaminergic neurons, particularly in animal models of Parkinson's disease and L-DOPA-induced dyskinesia [6-9]. Furthermore, preclinical and clinical trials have revealed a possible treatment for other diseases such as Fragile-X syndrome [10, 11], depression [12] and gastro-oesophageal reflux [13].

The classical approach in controlling the pharmacological activity of $mGlu_5$ involves the use of orthosteric agonists and antagonists, which compete with glutamate, the endogenous agonist. These orthosteric ligands, e.g. Quisqualate (**1**) [14] or (*S*)-MCPG (**2**) [15], bind to the $mGlu_5$ receptor extracellular domain but achieving suitable selectivity for one subtype over another is difficult because of the highly conserved orthosteric binding-site exhibited amongst mGlu-family members [16].

Allosteric modulators may solve this selectivity issue, since they bind to a less conserved allosteric site in the transmembrane domain, which shows more variation across subtypes [17]. Moreover, allosteric ligands, with lower polarity due to the higher hydrophobicity of the allosteric site, generally allow for better absorption [18] and more efficient crossing of the blood-brain barrier (BBB) [19]. Examples of such ligands include positive allosteric modulators (PAMs) CDPPB (**3**) [20] and VU0409551/JNJ-46778212 (**4**) [21]; and negative allosteric modulators (NAMs) fenobam (**5**) [22], MPEP

(**6**) [23], raseglurant (**7**) [24] and mavoglurant (**8**) [25], with the last having been recently co-crystallized in the allosteric pocket of the $mGlu_5$ transmembrane domain [26].

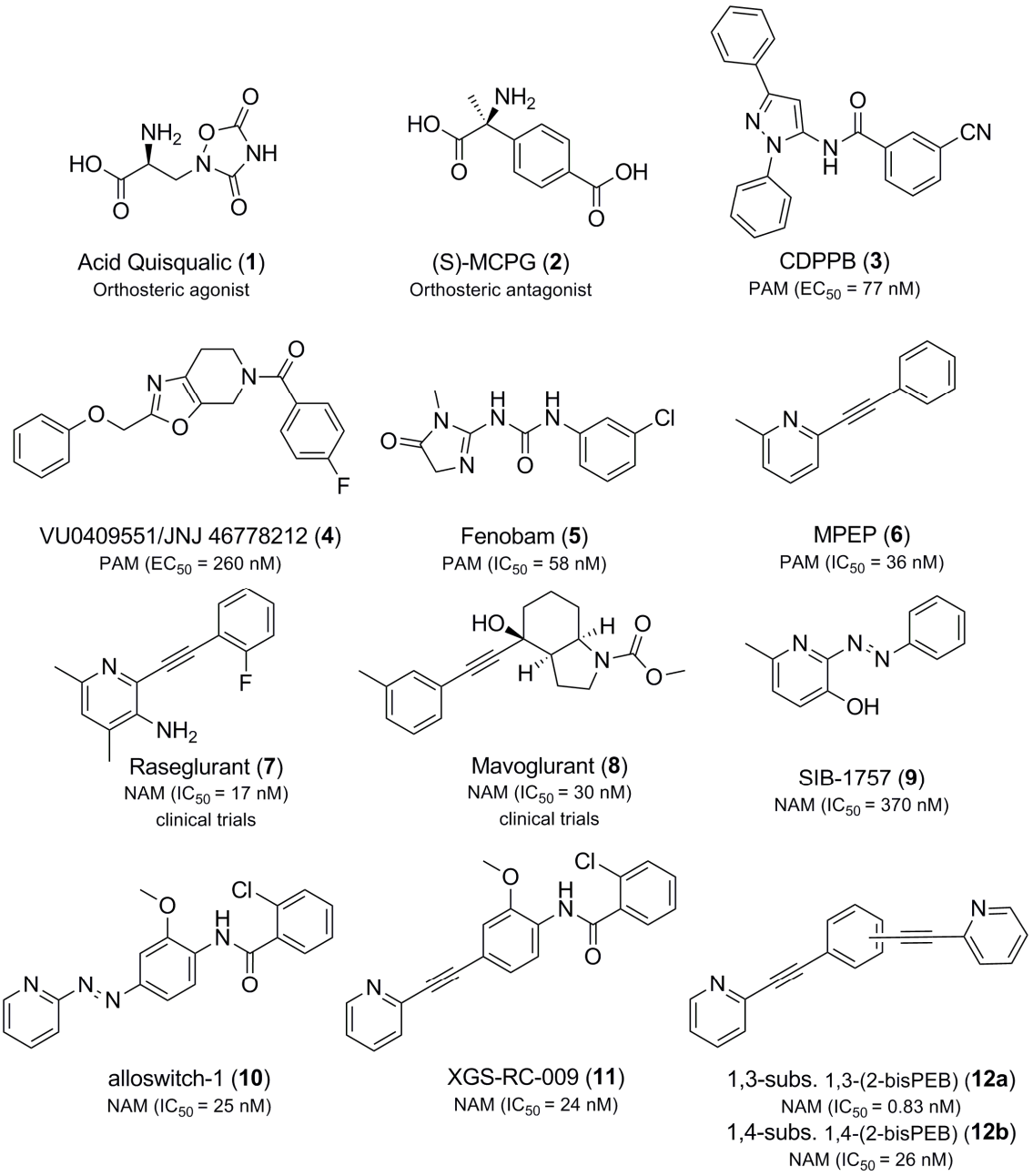

Figure 1. Examples of $mGlu_5$ ligands. Compound **1** is an orthosteric agonist [14], compound **2** is an orthosteric antagonist [15], compounds **3** and **4** are positive allosteric modulators (PAMs) and compounds **5**-**11** are negative allosteric modulators (NAMs) [22-25, 27-30]. Compounds **6**, **7**, **11**, **12a** and **12b** are 2-ethynylpyridine derivatives and compounds **9** and **10** are phenylazopyridine derivatives [20, 21].

Interestingly, many NAMs of $mGlu_5$, which usually display an inverse agonist activity, include a terminal pyridine or thiazole with an ethynyl unit at position 2 or 4, respectively [24]. According to recent publications [26, 31], this ethynyl moiety traverses a narrow channel in the allosteric site of the transmembrane domain, which might explain the predominance of the diaryl alkyne scaffold among $mGlu_5$ allosteric

modulators. However, the presence of a triple bond is not imperative for potent $mGlu_5$ PAMs and NAMs, since azo-bridged compounds such as SIB-1757 (**9**) are also $mGlu_5$ NAMs with potencies in the nanomolar range [27].

Recently we reported that alloswitch-1 (**10**), a photoswitchable $mGlu_5$ NAM with potency in the nanomolar range (IC_{50} = 25 nM) and containing a phenylazopyridine, displays reversible photoisomerization from *trans*- to *cis*-isomer [28], which can be translated to reversible activation-deactivation of $mGlu_5$ receptors in transfected cells, native cell cultures and *in vivo* [32].

In fact, *trans*-alloswitch-1 (**10**) most likely binds to the $mGlu_5$ receptor in a very similar fashion to mavoglurant (**8**) or MPEP (**6**), as we recently reported [33], whereas the binding of the *cis*-isomer is unstable or absent, in agreement with its lower observed activity [28]. In our computational simulations, the position of the azo-bond of the *trans* isomer occupies exactly the same narrow channel described by Doré et al. [26], sharing a common binding mode. In addition, alloswitch-1 (**10**) possesses a high structural resemblance to XGS-RC-009 (**11**), a recently reported potent (IC_{50} = 24 nM) $mGlu_5$ NAM [29], and only differs in the spacer between the western aromatic rings: an azo-bond for alloswitch-1 (**10**) and an ethynyl-bond for XGS-RC-009 (**11**). This further indicates the suitability of compounds containing either spacer type for achieving proper NAM activity in the $mGlu_5$ receptor.

In the present study, we confirm this correlation between azo-bonds and ethynyl-bonds for $mGlu_5$ NAMs from the functional and binding points of view. For that reason, we selected 1,3-(2-bisPEB) (**12a**) and 1,4-(2-bisPEB) (**12b**) [30], having considered their nanomolar NAM potency and their geometrically defined non-complex structure (*Figure 1*). Thus, we synthesised and characterised the corresponding azo-derivatives with the aim of obtaining new photoswitchable compounds for precise spatiotemporal control of the $mGlu_5$ receptor.

Results and Discussion

Chemistry

Previously reported compounds **12a** and **12b** [30] were prepared from 2-ethynylpyridine (**13**) and the corresponding diiodobenzene **14a**-**b** using a palladium catalysed Sonogashira coupling in moderate to good yields (*Scheme 1*). A two-step synthetic route yielded the azocompounds **19a** and **19b**, starting with a Sonogashira coupling of 2-chloropyridine **16** and the corresponding ethynyl aniline **15a**-**b** to give the intermediates **17a** and **17b** in moderate yields**.** The following Mills reaction of **17a** and **17b** with 2-nitrosopyridine **18** in acidic conditions gave compounds **19a** and **19b** in good yields. Finally, compounds **21a** and **21b** were also obtained by a single-step synthesis from the Mills reaction between 2-nitrosopyridine **18** and the corresponding diaminobenze **20a**-**b** in moderate to good yields.

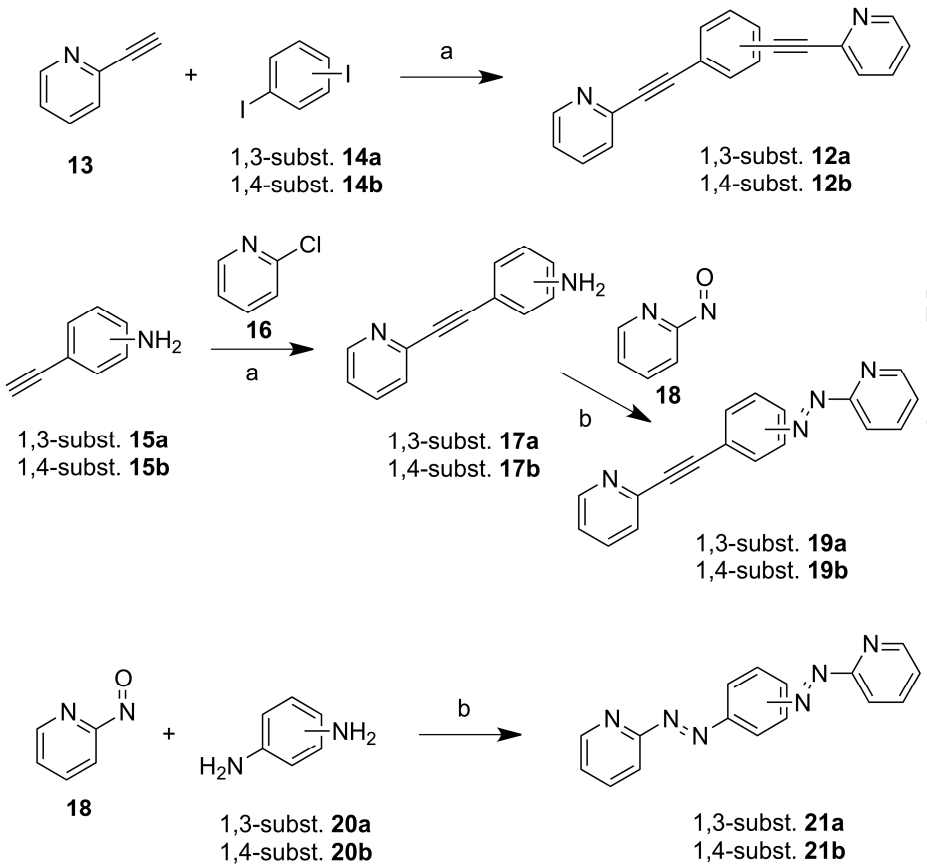

S**cheme 1**. Synthetic procedures for **12**, **17** and **19**. a) $PdCl_2(PPh_3)_2$, CuI, Et_3N, DMF, 50ºC, **12a** (87%), **12b** (47%), **15a** (30%), **15b** (23%); b) AcOH, DCM, r.t., **17a** (76%), **17b** (78%), **19a** (5%), **19b** (98%)

All the compounds were screened with high performance liquid chromatography (HPLC) coupled to a photodiode array detector (PDA) and a mass spectrometer (MS) to measure the UV-Vis absorption and mass spectra of the compounds (*supplementary material*). In addition, we were able to chromatographically separate and identify the *cis* and *trans* isomers of compounds **19a**, **19b**, **21a** and **21b**, since *cis*-isomers have a characteristic n-π* band at 420-440 nm and a displacement of the characteristic π-π* at shorter wavelengths (*supplementary material*).

Next, we tested the photoisomerization properties of azocompounds **19a-b** and **21a-b** with UV-Vis spectroscopy. In the absence of illumination we detected only the *trans*-isomer in all cases. To generate the *cis*-isomers we exposed the azocompound solution in acetonitrile to violet 380-nm-light since this wavelength is optimally located between the π-π* transition of the *trans* isomers and the minimum between π-π* and n-π* transitions of the *cis* isomers. Finally, 430-nm-light was used to recover the *trans* isomers since it is located in the centre of the n-π* transition of the *cis*-isomers. We were able to detect a nearly complete photoisomerisation of compound **19b**, since the profile of the UV-Vis spectrum obtained after violet illumination was the same as that obtained for the *cis* isomer peak detected by HPLC-PDA-MS (*supplementary material*). However, for compounds **19a** and **21a-b** we did not detect satisfactory photoisomerisation after illumination with violet light, in a similar manner to other previously reported bisazocompounds [34] (*supplementary material*). This indicates

that not all azo-compounds display a suitable photoisomerisation response for obtaining a high population of *cis* isomers under illumination, which is a necessary condition for efficient on/off receptor switching.

Pharmacology

We tested the compounds using an inositol phosphate (IP) accumulation assay in transiently transfected HEK293 cells with $mGlu_5$. Dose-response curves were generated to evaluate the antagonistic activity using the orthosteric agonist quisqualate and fenobam (**5**) as an $mGlu_5$ allosteric inverse agonist reference compound. Whilst compounds **12a** and **12b** were only tested in dark conditions, the corresponding incubations of compounds **19a**, **19b**, **21a** and **21b** were performed in parallel in both dark conditions and under 380-nm-illumination, to evaluate the photoswitching effect of these compounds on $mGlu_5$ receptor activity.

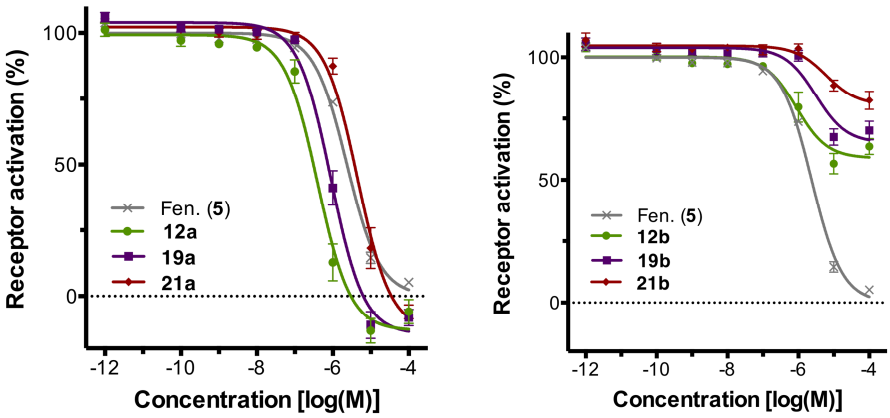

Figure 2. Dose-response curves of compounds **12a,b**, **19a,b**, and **21a,b** with fenobam (**5**) as control, obtained from IP accumulation assays with a constant concentration of quisqualate (100 nM) in dark conditions. The curves are normalised with respect to the response of fenobam, between 0% and 100%. Every point represents the mean of a minimum of three independent experiments with corresponding SEM as error bars.

The 1,3-disubstituted compounds **19a** and **21a** were found to be $mGlu_5$ NAMs. In comparison with fenobam (**5**), compound **19a** displayed better potency and efficacy whereas compound **21a** displayed higher efficacy but 2-fold lower potency. Both 19a and 21a showed similar efficacies to the structurally related compound **12a** (1,3-(2-BisPEB)), whose pharmacological properties were previously reported [30, 35]. The replacement of a triple bond in **12a** by an azo group in **19a** resulted in a 2-fold loss of potency in $mGlu_5$, a result which was also observed but to a greater extent (a 13-fold loss) when replacing both ethynyl spacers by N=N in **21a**.

The 1,4 substituted compounds **12b**, **19b** and **21b** also displayed NAM activity in $mGlu_5$, with lower potency than the corresponding 1,3-disubstituted compounds and, interestingly, with a much lower efficacy, signifying a partial antagonistic efficacy, which we have attributed to the different substitution pattern at the central benzene ring in the

2-ethynylpyridines or the 2-azopyridines, respectively (*Figure 2* and *Table 1*). Interestingly, 1,3-disubstituted compounds display a similar efficacy, or even a bit higher than fenobam (**5**), a classic allosteric inverse agonist [22], while 1,4-disubstituted compounds only partially antagonized the effect of quisqualate in $mGlu_5$. Moreover, the potencies (IC_{50}) of the 1,4-isomers were found to be within a similar range as the 1,3-isomers.

	IC_{50} ± SEM (µM)	Efficacy[a] ± SEM (%)	PPS[b]	PDE[c] (%)
12a	0.43±0.08	114±5	NT[d]	NT[d]
12b	1.21±0.40	42±4	NT[d]	NT[d]
19a	0.96±0.21	115±4	1.3	9
19b	3.09±0.27	35±4	2.9	15
21a	4.92±0.95	114±3	2.2	15
21b	6.13±0.16	19±4	1.2	-1
Fenobam	2.30±0.25	100±0	1.0	0

Table 1. Potency (IC_{50}) and efficacy of the series of compounds in $mGlu_5$, including photoinduced potency shift (PPS) of the IC_{50} and photoinduced difference of efficacy (PDE) between dark and illuminated conditions. Data extracted from dose-response curves obtained with an IP accumulation and constant 100 nM concentration of quisqualate. (a) Efficacy measured from bottom of the dose-response curve, normalised with respect to the response of fenobam between 0% and 100%. (b) PPS corresponds to the ratio of the IC_{50} in dark conditions and under violet illumination, (c) PDE corresponds to the difference in efficacy (%) between dark conditions and violet illumination, (d) NT: non-tested.

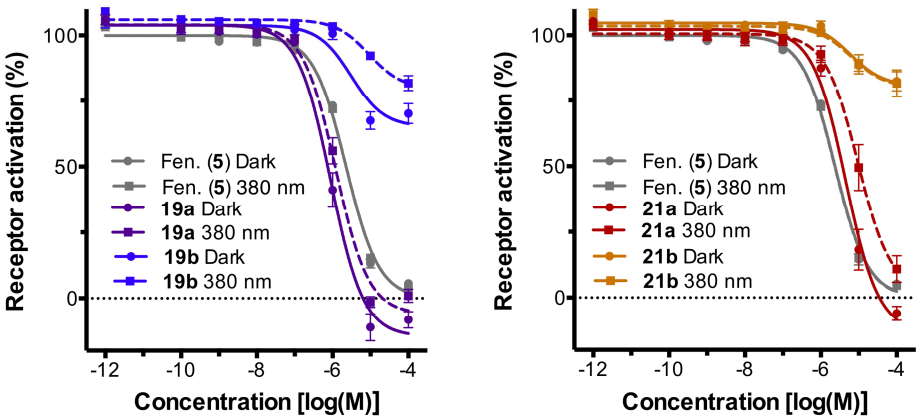

Figure 3. Dose-response curves of compounds **19a,b**, and **21a,b** obtained from IP accumulation assays with a constant concentration of quisqualate (100 nM) in dark conditions (plain line) and under illumination at 380 nm (dotted line). Every point represents the mean of a minimum of three independent replicates with corresponding SEM as error bars.

As anticipated from the photoisomerisation experiments, the response of the compounds tested under different illumination conditions was not efficient enough to provide a useful light-dependent control of $mGlu_5$ activity in cell assays. Upon

illumination at 380 nm, we detected successful receptor photoswitching behaviour for compound **19b**, which was a partial antagonist as a *trans*-isomer but experiences a 3-fold loss in potency and 15% loss in efficacy under violet illumination (mainly *cis*-isomer) (*Figure 3* and *Table 1*). The photoinduced potency shifts (PPS) [36] of the dose response curves with the azo-compounds **19a** and **21a,b** were not sufficient to achieve useful on/off receptor photoswitching. This result was probably due to the compounds intrinsic molecular photochemical properties, which do not allow for a clear-cut difference in the induction of different populations of the *cis*/*trans* isomers at the wavelengths used. Another possible explanation for this lack of photoactivity could be an insufficient difference in the affinity of the *cis* and *trans* isomers for the receptor, which would result in low stability of the on/off states upon binding. This reflects the necessary combination of photochemical and pharmacological properties of the azo compounds for achieving an effective photoswitching of receptor activity in cell assays or *in vivo* applications [36].

After examination of the results obtained, we were particularly interested in the reasons behind the $mGlu_5$ efficacy differences observed for the 1,4 and 1,3 positional isomers (measured by the asymptotic minimum effects of the dose-response curves on the y-axis), which occur without significantly altering their location along the x-axis (IC_{50} values). We hypothesized that this could be due to different binding modes in the transmembrane domain of the $mGlu_5$ receptor. The high homology between isomers and similarity of the *trans*-azo and ethynyl bonds, both from the structural and geometrical points of view, result in compounds with very rigid scaffolds where the aromatic rings are either in angular or linear arrangements. Therefore, the binding modes of each geometrical type may be significantly different, since these molecules do not have the flexibility needed to rearrange their scaffold in order to bind in the same pose in the same receptor pocket. To verify this hypothesis, we performed some computational docking.

In silico binding model

To explore the possible binding modes of compounds **12a-b**, **19a-b** and **21a-b**, each compound was docked into the crystal structure of $mGlu_5$ (PDB id 4OO9, minus its mavoglurant co-crystallized ligand). For each respective docking, the top-ranked protein-ligand complex was energy-minimized to optimize intermolecular interactions.

From the results shown in *Figure 4*, the 1,3-compounds are able to bind at the bottom of the allosteric pocket because their structures are easily accommodated within the distinctive angular binding-site, displaying a similar binding pose to the previously co-crystallized $mGlu_5$ NAMs: mavoglurant (in PDB id 4OO9 [26]) and HTL14242 (in PDB id 5CGD [37]). In doing so, each 1,3-compound achieves a favourable docking score (*Table 2*), making an H-bond with S809 on TM7 (after energy minimization), and in the case of **19a** and **21a**, an additional H-bond with N747 on TM5. However, the 1,4-compounds are unable to bind at the bottom of the allosteric pocket (at least in the $mGlu_5$ crystal structure of PDB id 4OO9), as they are unable to accommodate their

structures within the angular binding-site. Instead, they bind higher in the pocket with a pose similar to that observed with the co-crystallized ligand FITM in the crystal structure of $mGlu_1$ (PDB id: 4OR2 [38]). As a result of this higher binding pose, the 1,4-compounds achieve much less favourable docking scores (*Table 3*) and are unable to make an H-bond with S809 on TM7 or any other residue in the allosteric pocket. Although this higher binding pose is apparently functional in terms of $mGlu_1$ allosterism, it is unlikely to be functional in $mGlu_5$, as reflected by the low docking scores observed here (indicating a poor fit) and by experimental data (including current $mGlu_5$ crystal structures) [26, 37], which suggests S809 interaction is critical for correct $mGlu_5$ NAM functionality [35].

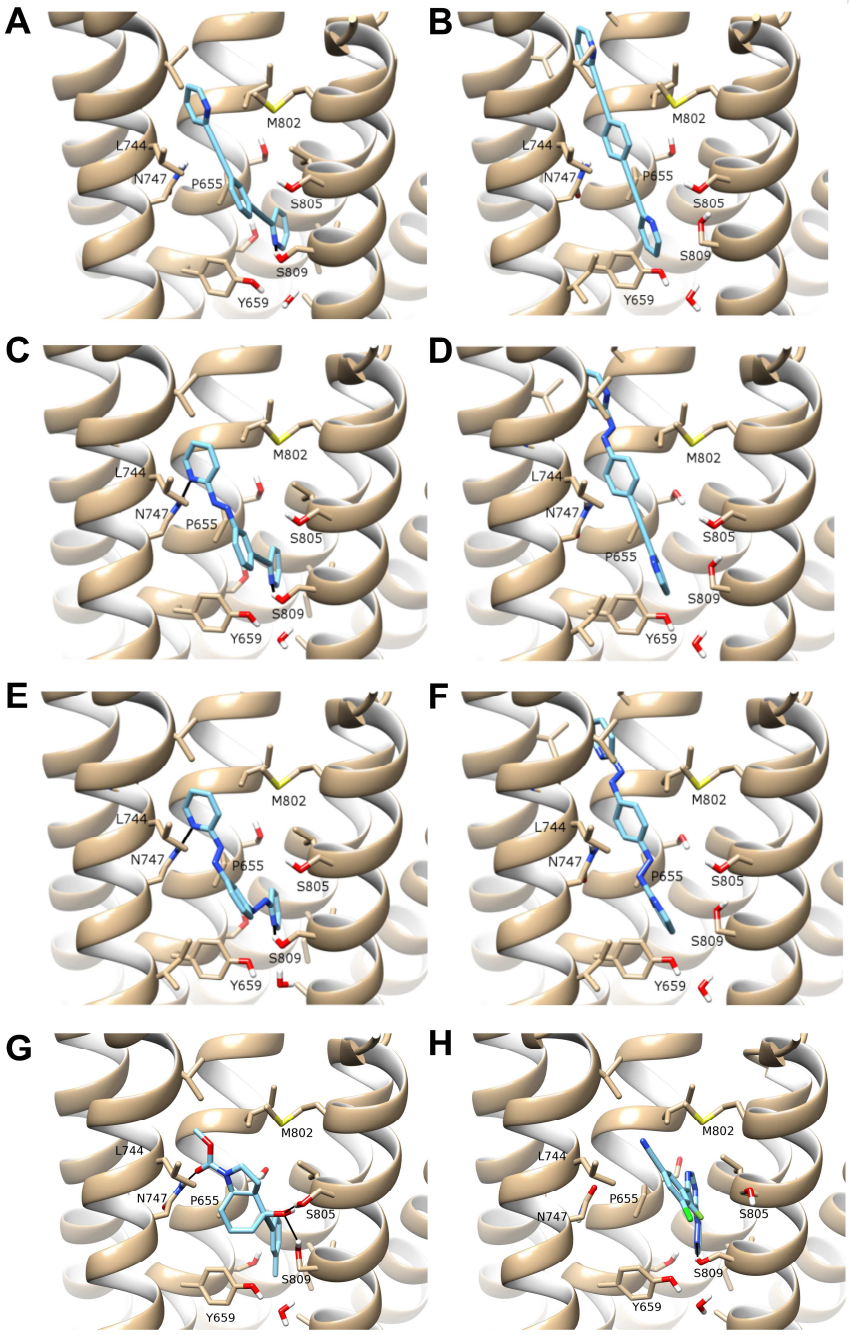

Figure 4. Six compounds docked into crystal structure of $mGlu_5$ receptor (PDB id 4OO9) using AutoDock4.2: (A) **12a**, (B) **12b**, (C) **19a**, (D) **19b**, (E) **21a**, (F) **21b** and, for comparison, co-crystallized: (G) mavoglurant (PDB id 4OO9) and (H) HTL14242 (PDB id 5CGC). Ligands are shown in cyan, receptor in beige, and protein-ligand H-bonds as black lines. The allosteric binding pocket is shown from the side with selected residues labelled (TM5 front-left, TM7 front-right, TM3 central, TM4 background-left, TM2 background-right, TM6 invisible).

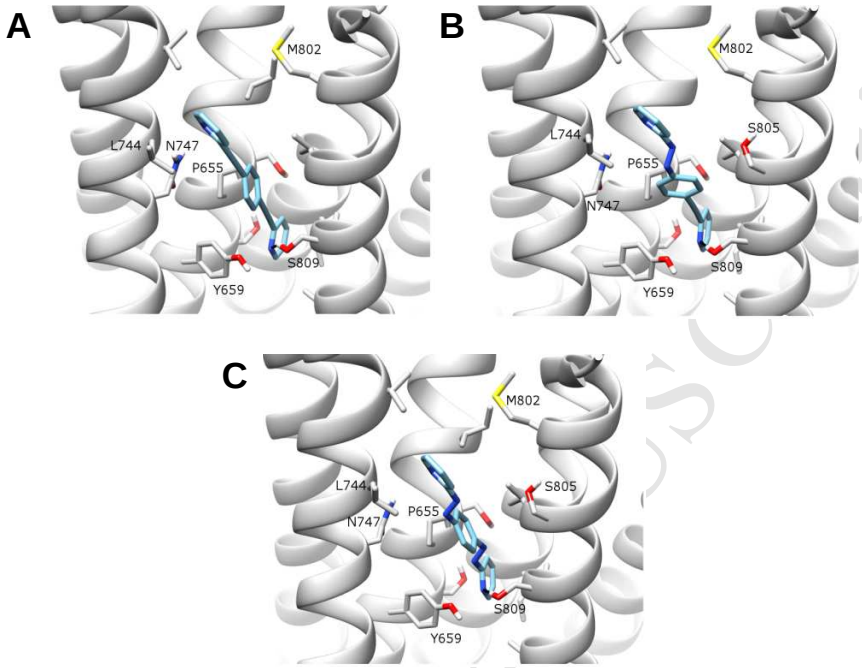

Figure 5. Linear-shaped 1,4-compounds: (A) **12b**, (B) **19b**, (C) **21b** re-docked into an alternative receptor conformation of $mGlu_5$, derived from original crystal structure (PDB id 4OO9). Ligands are shown in cyan, receptor in grey, and protein-ligand H-bonds as black lines. The allosteric binding pocket is shown from the side with selected residues labelled (TM5 front-left, TM7 front-right, TM3 central, TM4 background-left, TM2 background-right, TM6 invisible).

	Docking Score in $mGlu_5$ crystal 4OO9 (Predicted Ki, nM)	Docking Score in alternative $mGlu_5$ conformation (Predicted Ki, nM)
12a	437.77	-
12b	9000.15	1000.27
17a	124.13	-
17b	817.74	405.60
19a	140.54	-
19b	768.31	373.97

Table 2. Docking scores for six compounds in two conformations of $mGlu_5$ (original crystal structure and a computationally-generated alternative). Three angular-shaped 1,3-compounds: **12a**, **19a** and **21a**, and three linear 1,4-compounds: **12b**, **19b** and **21b**.

In recognition of the fact that GPCRs are flexible dynamic receptors, an alternative conformation of $mGlu_5$ was utilised to re-dock the 1,4-compounds in an attempt to

identify better binding poses at the bottom of the allosteric pocket (more similar in nature to current co-crystallized $mGlu_5$ NAMs). This alternative receptor conformation was derived from the original $mGlu_5$ crystal structure (PDB id 4OO9) through computational conformational sampling performed previously [33]. This process results in a relatively subtle adjustment of side-chain packing between TM6 and TM7 but, more significantly, an enlargement and alteration of the binding pocket from an angular shape to a wider linear shape. Using this alternative receptor conformation, the 1,4-compounds instead dock at the bottom of the allosteric pocket, making an H-bond with S809 on TM7 (*Figure 5*), the residue designated as important for interaction with $mGlu_5$ NAMs [35], and packing against hydrophobic residues on TM5 (e.g. L744) and TM6. In accordance with this changed binding-mode, the docking scores of the 1,4-compounds are improved compared to the previous dockings in the original crystal structure (PDB id 4OO9) (*Table 2*). However, it should be noted that this alternative receptor conformation is perhaps not as readily accessible in energetic terms as the original crystal structure conformation, potentially affecting the pharmacological activity of the 1,4-compounds.

Concluding remarks

We synthesised four derivatives of the $mGlu_5$ NAMs 1,3-(2-BisPEB) and 1,4-(2-BisPEB) via azologisation [39] of one or two ethynyl groups, which maintain similar pharmacological properties to the previous reported isosteres [30], including similar potencies.

Despite the similar potencies among the compounds tested, we found substantial differences in their antagonistic efficacies on the $mGlu_5$ receptor: compounds with 1,3-substitution displayed an inverse agonist efficacy similar to the reference compound fenobam, whereas compounds with 1,4-substitution displayed partial antagonistic effects.

Computational docking in the $mGlu_5$ crystal structure [26] revealed the angular-shaped 1,3-substituted compounds bind in a very similar pose to the co-crystallised inverse agonist mavoglurant, whereas the linear 1,4-substituted compounds bind in a different pose, unlikely to be functional and with a concomitantly worse docking score. However, an alternative conformation of the $mGlu_5$ transmembrane domain might adapt to these linear-shaped compounds in a functional-like pose, which may be responsible for their partial antagonism behaviour.

The discovery of a molecular switch from full allosteric inverse agonists to partial allosteric antagonists is of high interest, since recent publications have reported the advantageous properties of partial $mGlu_5$ NAMs [40, 41], which might avoid on-target side-effects of full $mGlu_5$ inhibition by classical allosteric inverse agonists [42, 43]. Therefore, our approach based on changing substituent positions of molecularly rigid

$mGlu_5$ NAMs may be useful for discovering new partial $mGlu_5$ NAMs with safer pharmacological profiles and better drug design outcomes.

Experimental Section

Chemistry

All the chemicals and solvents were provided from commercial suppliers and used without purification, except the anhydrous solvents, which were treated previously through a system of solvent purification (*PureSolv*), degasified with inert gases and dried over alumina or molecular sieve (DMF). Dimethylisopropylamine (DMAP) and triethylamine (TEA) were also dried over alumina. Compounds **12a-b**, **19a-b**, and **21a-b** were synthesized according to the protocols described below. Reactions were monitored by thin layer chromatography (60F, 0.2 mm, *Macherey-Nagel*) by visualisation under 254 and/or 365 nm lamp. *Flash* column chromatography was performed with SNAP KP-Sil 50 µm (*Biotage*) or SNAP KP-C18-HS 50 µm (*Biotage*) columns, automated with *Isolera One* with UV-Vis detection (*Biotage*). Melting points (mp) were determined with a *Büchi B-545*, ramp 2 ºC/min. Nuclear magnetic resonance (NMR) spectra were determined with *Variant-Mercury* 400 MHz (*Agilent Technologies*). Chemical shifts are reported in parts per million (ppm) against the reference compound using the signal of the residual non-deuterated solvent (Chloroform δ = 7.26 ppm (^{1}H), δ = 77.16 ppm (^{13}C), DMSO δ = 2.50 ppm (^{1}H)). Purity determination and absorption UV-Vis spectra were determined with High-Performance Liquid Chromatography Thermo Ultimate 3000SD (*Thermo Scientific Dionex*) coupled to a photodiode array detector and a mass spectrometer LTQ XL ESI-ion trap (*Thermo Scientific*) (HPLC-PDA-MS); 5 µL of sample 0.25 mM in a mixture DMSO/AcN 1:9 were injected, using an Acquity UPLC BEH C18 column (*Waters*) 1.7 µm 2.1x100 mm (SN 021532354157 76) at 30ºC. The mobile phase used was a mixture of A = NH_4HCO_3 aqueous buffer 10 mM pH=7.4 and B = acetonitrile (AcN) with the method described as follows: flow 0.3 mL/min, 5%B-100%B 3 min, 100%B 5 min, total runtime 15 min; purity is given as % of absorbance of the *cis* and *trans* isomers at 254 nm; UV-Vis spectra were collected every 0.2 s between 650 and 275 nm and bands are % of maximal absorbance; data from mass spectra were analysed by electrospray ionization in positive and negative mode every 0.3 s between 50 and 1000 Da and peaks are given m/z (% of basis peak). High-resolution mass spectra (HRMS) and elemental composition were analysed by FIA (flux injected analysis) with ultra-high performance liquid chromatography (UPLC) *Aquity* (*Waters*) coupled to LCT Premier orthogonal accelerated time of flight mass spectrometer (TOF) (*Waters*). Data from mass spectra were analysed by electrospray ionization in positive and negative mode. Spectra were scanned between 50 and 1500 Da with values every 0.2 s and peaks are given m/z (% of basis peak).

1,3-bis(pyridin-2-ylethynyl)benzene 12a: General procedure A: 2-ethylpyridine **13** (35 µL, 0.35 mmol) and dry diisopropylethylamine (DIPEA) (0.1 ml, 0.57 mmol) were

added to a dispersion of 1,3-diiodobenzene **14a** (46 mg, 0.14 mmol), copper(I) iodide (2 mg, 0.01 mmol) and bis(triphenylphosphine) palladium (II) chloride (5.4 mg, 0.01 mmol) in dry dimethyl formamide (DMF) (1 mL) in a *Schlenk* flask with argon atmosphere at room temperature. The mixture was stirred at 50ºC for 5 hours. The reaction mixture was diluted in EtOAc (15 mL) and washed with aqueous Na_2CO_3 1 N (10 mL), saturated $NaHCO_3$ (10 mL), water (10 mL) and brine (10 mL), dried over anhydrous MgSO4, filtered and concentrated *in vacuo*. The residue was purified through *flash* chromatography using *Biotage Isolera* equipment (SNAP KP-C18-HS 12g, A=H_2O, B=MeCN; 0%B 5CV, 0%B-1%B 2CV, 1%B-4%B 2.5 CV, 4%B 1.5CV, 4%B-7%B 6CV, 7%B-9%B 0.5CV, 9%B-100%B 2 CV, 100%B 5CV). The title product **12a** was obtained as brown colour solid (34 mg) with an 87% yield, mp 89.9-91.3ºC. ^{1}H NMR (400 MHz, $CDCl_3$) δ 8.65 (br, 2H), 7.82 (t, J = 1.6 Hz, 1H), 7.70 (td, J = 7.7, 1.6 Hz, 2H), 7.60 (dd, J = 7.8, 1.6 Hz, 2H), 7.54 (d, J = 7.9 Hz, 2H), 7.37 (t, J = 7.7 Hz, 1H), 7.31 – 7.22 (m, 2H). ^{13}C NMR (101 MHz, $CDCl_3$) δ 150.12, 143.22, 136.43, 135.42, 132.58, 128.76, 127.51, 123.16, 122.86, 89.33, 88.37. HPLC-PDA-MS: RT = 5.91 min, 99.87% (254 nm), PDA λ_{max} = 296 nm, MS (m/z) $[M+H]^+$ 280.94.

1,4-bis(pyridin-2-ylethynyl)benzene 12b: General procedure A was used with **13** (36 µL, 0.36 mmol) and dry DIPEA (0.1 ml, 0.57 mmol) and 1,4-diiodobenzene **14b** (47 mg, 0.14 mmol), CuI (2 mg, 0.01 mmol) and $PdCl_2(PPh_3)_2$ (5.4 mg, 0.01 mmol) in DMF (1 mL). The residue was purified through *flash* chromatography using *Biotage Isolera* equipment (SNAP KP-C18-HS 12g, A= H_2O B=MeCN; 0%B 5CV, 0%B-1%B 2CV, 1%B-4%B 2.5 CV, 4%B 1.5CV, 4%B-7%B 6CV, 7%B-9%B 0.5CV, 9%B-100%B 2 CV, 100%B 5CV). The title product **12b** was obtained as cream colour solid (18 mg) with a 45% yield, mp 187.9-188.1ºC. ^{1}H NMR (400 MHz, $CDCl_3$) δ 8.65 (br, 2H), 7.72 (td, J = 7.7, 1.6 Hz, 2H), 7.60 (s, 4H), 7.56 (d, J = 8.0 Hz, 2H), 7.28 (dd, J = 6.9, 5.3 Hz, 2H). ^{13}C NMR (101 MHz, $CDCl_3$) δ 150.00, 143.08, 136.62, 132.18, 127.56, 123.23, 122.96, 90.55, 89.24. HPLC-PDA-MS: RT = 5.89 min, 99.72% (254 nm), PDA λ_{max} = 319 nm, MS (m/z) $[M+H]^+$ 280.91.

3-(pyridin-2-ylethynyl)aniline 17a: General procedure B: 2-chloropyridine **16** (0.13 mL, 1.37 mmol), 3-ethynylaniline **15a** (0.24 mL, 2.13 mmol) and dry triethylamine (TEA) (0.76 ml, 5.46 mmol) were added to a dispersion of copper(I) iodide (13 mg, 0.07 mmol) and bis(triphenylphosphine) palladium (II) chloride (48 mg, 0.07 mmol) in dry dimethyl formamide (DMF) (8 mL) in a *Schlenk* flask with argon atmosphere at room temperature. The mixture was stirred at 60ºC for 4 hours. The reaction mixture was diluted in EtOAc (100 mL) and washed with aqueous Na_2CO_3 1 N (50 mL), saturated $NaHCO_3$ (50 mL), water (50 mL) and brine (50 mL), dried over anhydrous MgSO4, filtered and concentrated *in vacuo*. The residue was purified through silica *flash* chromatography (DCM and DCM + 1% MeOH) to afford the title compound **17a** as brown thick oil (80 mg, 30% yield). ^{1}H NMR (400 MHz, $CDCl_3$) δ 8.61 (ddd, J = 4.9, 1.8, 1.0 Hz, 1H), 7.67 (td, J = 7.7, 1.8 Hz, 1H), 7.50 (dt, J = 7.9, 1.1 Hz, 1H), 7.23 (ddd, J = 7.6, 4.9, 1.2 Hz, 1H), 7.14 (t, J = 7.8 Hz, 1H), 7.00 (dt, J = 7.6, 1.2 Hz, 1H), 6.91 (dd, J = 2.4, 1.5 Hz, 1H), 6.69 (ddd, J = 8.1, 2.4, 1.0 Hz, 1H), 3.13 (br, 2H). ^{13}C NMR (101

MHz, CDCl3) δ 150.11, 146.42, 143.65, 136.31, 129.45, 127.30, 123.02, 122.79, 122.62, 118.30, 116.17, 89.80, 88.09. HRMS (m/z): $[M+H]^+$ calculated for $C_{13}H_{11}N_2$, 195.0922; found, 195.0922.

2-((3-(pyridin-2-yldiazenyl)phenyl)ethynyl)pyridine 19a: General procedure C: One drop of acetic acid was added to a solution of 2-nitrosopyridne **18** (15 mg, 0.14 mmol) and aniline **17a** (18 mg, 0.09 mmol) in DCM (1 mL) and the resulting solution was left stirring at room temperature for 3 days. The reaction mixture was concentrated *in vacuo* and the remains of acetic acid were co-evaporated with toluene twice. The obtained residue was purified through *flash* chromatography using *Biotage Isolera* equipment (SNAP KP-C18-HS 12g, A= H_2O B=MeOH; 0%B 3CV, 0%B-60%B 5CV, 60%B-85%B 8CV, 85%B-100%B 1CV, 100%B 4CV). The title product **19a** was obtained (20 mg, orange solid) with a 76% yield, mp 79.1-79.8 ºC. ^{1}H NMR (400 MHz, $CDCl_3$) δ 8.76 (ddd, J = 4.8, 1.8, 0.9 Hz, 1H), 8.65 (ddd, J = 5.0, 1.8, 0.9 Hz, 1H), 8.31 – 8.25 (m, 1H), 8.08 (ddd, J = 8.1, 2.0, 1.2 Hz, 1H), 7.93 (ddd, J = 8.0, 7.3, 1.8 Hz, 1H), 7.85 (dt, J = 8.0, 1.1 Hz, 1H), 7.77 (dt, J = 7.7, 1.3 Hz, 1H), 7.75 (td, J = 7.7, 1.8 Hz, 1H), 7.58 (dt, J = 7.6, 0.9 Hz, 1H), 7.54 (t, J = 7.9 Hz, 1H), 7.43 (ddd, J = 7.3, 4.8, 1.2 Hz, 1H), 7.31 (ddd, J = 7.6, 4.9, 1.2 Hz, 1H). ^{13}C NMR (101 MHz, $CDCl_3$) δ 162.73, 152.36, 149.74, 149.67, 142.76, 138.60, 136.99, 135.45, 129.51, 127.65, 127.02, 125.70, 124.59, 123.38, 123.27, 116.09, 89.32, 88.91. HPLC-PDA-MS: RT = 5.50 min, 21.53% (254 nm), PDA λ_{max} = 290, 428 nm, MS (m/z) $[M+H]^+$ 284.96 (*cis*-isomer); RT = 5.76 min, 78.00% (254 nm), PDA λ_{max} = 302. 446 nm, MS (m/z) $[M+H]^+$ 284.95 (*trans*-isomer). HRMS (m/z): $[M+H]^+$ calculated for $C_{18}H_{13}N_4$, 285.1145; found, 285.1140.

4-(pyridin-2-ylethynyl)aniline 17b: General procedure B was used with **16** (0.13 mL, 1.37 mmol), dry TEA (0.76 ml, 5.46 mmol), 4-ethynylaniline **15b** (249 mg, 2.05 mmol), CuI (13 mg, 0.07 mmol) and $PdCl_2(PPh_3)_2$ (48 mg, 0.07 mmol) in DMF (8 mL). The residue was purified through silica *flash* chromatography (DCM/hexanes 9:1, DCM, DCM + 0.5% MeOH and DCM + 1% MeOH) to afford the title compound **17b** as brown thick oil (60 mg, 23% yield). ^{1}H NMR (400 MHz, $CDCl_3$) δ 8.58 (ddd, J = 4.9, 1.9, 1.0 Hz, 1H), 7.64 (td, J = 7.7, 1.8 Hz, 1H), 7.47 (dt, J = 7.9, 1.1 Hz, 1H), 7.40 (d, J = 8.7 Hz, 2H), 7.18 (ddd, J = 7.6, 4.9, 1.2 Hz, 1H), 6.63 (d, J = 8.7 Hz, 2H), 3.48 (br, 2H). ^{13}C NMR (101 MHz, $CDCl_3$) δ 150.02, 147.46, 144.18, 136.20, 133.67, 126.88, 122.26, 114.78, 111.51, 90.69, 87.10. HRMS (m/z): $[M+H]^+$ calculated for $C_{13}H_{11}N_2$, 195.0922; found, 195.0923.

2-((4-(pyridin-2-yldiazenyl)phenyl)ethynyl)pyridine 19b: General procedure C was used with one drop of AcOH, **18** (11 mg, 0.10 mmol) and **17b** (13 mg, 0.07 mmol) in DCM (1 mL). The obtained residue was purified through *flash* chromatography using *Biotage Isolera* equipment (SNAP KP-C18-HS 12g, A= H_2O B=MeOH; 0%B 3CV, 0%B-60%B 5CV, 60%B-85%B 8CV, 85%B-100%B 1CV, 100%B 8CV). The title product **19b** was obtained (15 mg, orange solid) with a 78% yield, mp 185.9-186.6ºC. ^{1}H NMR (400 MHz, $CDCl_3$ NMR) δ 8.76 (ddd, J = 4.8, 1.8, 0.8 Hz, 1H), 8.65 (ddd, J = 4.9, 1.8, 0.9 Hz, 1H), 8.06 (d, J = 8.6 Hz, 2H), 7.93 (ddd, J = 8.0, 7.3, 1.9 Hz, 1H), 7.85

(dt, J = 8.0, 1.1 Hz, 1H), 7.77 (d, J = 8.6 Hz, 2H), 7.73 (dd, J = 7.7, 1.8 Hz, 1H), 7.58 (dt, J = 7.9, 1.1 Hz, 1H), 7.43 (ddd, J = 7.3, 4.7, 1.2 Hz, 1H), 7.30 (ddd, J = 7.7, 4.9, 1.2 Hz, 1H). ^{13}C NMR (101 MHz, $CDCl_3$) δ 162.86, 152.17, 149.94, 149.76, 142.86, 138.57, 136.79, 133.14, 127.62, 126.08, 125.65, 123.79, 123.33, 116.16, 91.06, 89.43. HPLC-PDA-MS: RT = 5.48 min, 19.34% (254 nm), PDA λ_{max} = 307, 435 nm, MS (m/z) $[M+H]^+$ 284.95 (*cis*-isomer); RT = 5.75 min, 80.09% (254 nm), PDA λ_{max} = 349, 443 nm, MS (m/z) $[M+H]^+$ 284.96 (*trans*-isomer). HRMS (m/z): $[M+H]^+$ calculated for $C_{18}H_{13}N_4$, 285.1140; found, 285.1140.

1**,3-bis(pyridin-2-yldiazenyl)benzene 21a:** General procedure C was used with two drops of AcOH added to **16** (120 mg, 1.11 mmol) and benzene-1,3-diamine **20a** (40 mg, 0.37 mmol) in DCM (10 mL). The obtained residue was purified through *flash* chromatography using *Biotage Isolera* equipment (SNAP KP-C18-HS 12g, A= H_2O B=MeOH; 5%B 4CV, 5%B-50%B 3CV, 50%B-10%B 8CV, 100%B 6CV). The title product **21a** was obtained as a dark solid (5 mg) with a 5% yield, mp 101.3-101.9ºC. ^{1}H NMR (400 MHz, $CDCl_3$) δ 8.77 (ddd, J = 4.8, 1.8, 0.9 Hz, 2H), 8.70 (t, J = 2.0 Hz, 1H), 8.25 (dd, J = 7.9, 2.0 Hz, 2H), 7.95 (ddd, J = 8.0, 7.2, 1.8 Hz, 2H), 7.89 (dt, J = 8.0, 1.1 Hz, 2H), 7.73 (t, J = 7.9 Hz, 1H), 7.45 (ddd, J = 7.2, 4.8, 1.3 Hz, 2H). ^{13}C NMR (101 MHz, $CDCl_3$) δ 162.79, 153.33, 149.80, 138.61, 130.01, 127.09, 125.74, 118.01, 116.37. HPLC-PDA-MS: RT = 5.11 min, 3.65% (254 nm), PDA λ_{max} = 278, 428 nm, MS (m/z) $[M+H]^+$ 288.93 (*cis-cis*-isomer); RT = 5.34 min, 24.86% (254 nm), PDA λ_{max} = 314, 432 nm, MS (m/z) $[M+H]^+$ 288.95 (*cis-trans*-isomer); RT = 5.60 min, 70.71% (254 nm), PDA λ_{max} = 319, 443 nm, MS (m/z) $[M+H]^+$ 288.96 (*trans-trans*-isomer). HRMS (m/z): $[M+H]^+$ calculated for $C_{16}H_{13}N_6$, 289.1202; found, 289.1216.

1**,4-bis(pyridin-2-yldiazenyl)benzene 21b:** General procedure C was used with two drops of AcOH, **18** (33 mg, 0.31 mmol) and benzene-1,4-diamine **20b** (15 mg, 0.14 mmol) in DCM (1 mL). The title product **21b** (39 mg, orange solid) was afforded with a 98% yield, mp 211.6-212.7ºC. ^{1}H NMR (400 MHz, $CDCl_3$) δ 8.78 (d, J = 3.4 Hz, 2H), 8.22 (s, 4H), 7.96 (td, J = 7.7, 1.8 Hz, 2H), 7.89 (d, J = 7.9 Hz, 2H), 7.46 (ddd, J = 7.4, 4.8, 1.3 Hz, 2H). ^{13}C NMR (101 MHz, $CDCl_3$) δ 162.72, 154.18, 149.71, 138.73, 125.85, 124.70, 116.27. HPLC-PDA-MS: RT = 5.34 min, 5.33% (254 nm), PDA λ_{max} = 336, 437 nm, MS (m/z) $[M+H]^+$ 288.89 (*cis-trans*-isomer); RT = 5.59 min, 90.61% (254 nm), PDA λ_{max} = 353, 456 nm, MS (m/z) $[M+H]^+$ 288.90 (*trans-trans*-isomer), HRMS (m/z): $[M+H]^+$ calculated for $C_{15}H_{13}N_6$, 289.1202; found, 289.1216.

Pharmacology

HEK 293 cells were cultured and transfected by electroporation as previously described for expression of all rat mGlu receptors [44]. To maintain ambient glutamate at minimal concentrations, the excitatory amino acid transporter 1 (EAAC1) was co-transfected. All receptors contained an HA tag in their *N*-terminus to monitor their cell surface expression by ELISA. Once transfected, cells were seeded in black clear-bottom 96-well plates at a concentration of 1.5 × 105 cells/well. At least 4h before the experiment, we changed the medium to glutamate-free DMEM GlutaMAX-I (*Thermo*

Fisher Scientific). The day after, we estimated IP accumulation using the IP-One HTRF kit (*Cisbio Bioassays*) according to the manufacturer's instructions. Cells were stimulated to induce IP accumulation while being treated with test compounds for 30 min, at 37°C and 5% CO_2, and placed over an LED plate [28] (*FCTecnics*) at a distance of 2–3 cm for continuous illumination. To allow stimulation in both dark conditions and violet light illumination, two-thirds of the 96-well plate bottom was covered with aluminium foil. To avoid effects derived from the fast relaxation of azo-compounds in aqueous solution after the 30-min stimulation, we washed cells once in stimulation buffer alone before continuing with the lysis step of the assay protocol. For fluorescence readings with a RUBYstar HTRF HTS microplate reader (*BMG Labtech*), we transferred cell lysates to a black opaque-bottom 96-well plate. Dose-response data from IP accumulation assays were first normalized by the dose-response to reference allosteric modulator fenobam in both dark and illuminated conditions and then fitted with a standard Hill equation using GraphPad Prism version 6.0.

Computational

The molecular structures of six compounds: **12a-b**, **19a-b**, **21a-b** in *trans*-isomer state were constructed with Maestro version 9.8 (*Schrödinger Release 2014*). Each compound was docked into the transmembrane domain crystal structure of $mGlu_5$ (PDB id 4OO9, minus co-crystallized mavoglurant) using AutoDock4.2 with default parameters [45]. For each respective docked compound, the top-ranked complex (according to AutoDock docking score) was energy-minimized in the Amber14SB force-field [46] using CHIMERA [47] to optimize protein-ligand interactions. The three linear 1,4-compounds in *trans*-isomer state: **12b**, **19b** and **21b** were also docked (using same parameters) into an alternative $mGlu_5$ receptor conformation, previously derived from the $mGlu_5$ crystal structure (PDB id 4OO9) by using a conformational sampling technique [33].

Acknowledgments

This research has been supported by RecerCaixa foundation (2010ACUP00378 to P.G., J.G., and A.L.), the Marató de TV3 Foundation (110230 to J.G., 110231 to A.L., 110232 to C.G., and 111531 to P.G.), the Catalan government (2010 BP-A00194 to X.R., 2012 CTP 00033 and 2012 BE1 00597 to X.G.-S., 2014SGR-1251 to P.G., and 2014SGR-00109 to A.L.), the Spanish Government (CTQ2014-57020-R and PCIN-2013-017-C03-01 to A.L., and SAF2014-58396-R and PCIN-2013-018-C03-02 to J.G.), and the ERANET Neuron LIGHTPAINProject (to A.L., J.G., and J.-P.P.); SynBio MODULIGHTOR, Human Brain Project WAVESCALES and Ramón Areces foundation grants (to P.G.); the Agence Nationale de la Recherche (ANR-16-CE16-0010 to A.L. and C.G.).

Contributions

A.L. conceived and supervised the project. A.L., J.G., X.G.-S, X.R., J.D., P.G., C.G., and J.-P.P. designed experiments. X.G.-S., J.D., J.G. and A.L. designed compounds.

X.G.-S. synthesized the compounds, characterized their photoisomerisation and performed pharmacological assays. X.R., C.G. and J.-P.P analysed pharmacological results. J.D. performed the computational dockings. X.G.-S., J.D., J.G. and A.L. wrote the paper. All authors made corrections and approved the final manuscript.

References

[1] P.J. Conn, Physiological roles and therapeutic potential of metabotropic glutamate receptors, Ann. N. Y. Acad. Sci., 1003 (2003) 12-21.
[2] F. Nicoletti, J. Bockaert, G.L. Collingridge, P.J. Conn, F. Ferraguti, D.D. Schoepp, J.T. Wroblewski, J.P. Pin, Metabotropic glutamate receptors: from the workbench to the bedside, Neuropharmacol., 60 (2011) 1017-1041.
[3] J.P. Pin, F. Acher, The metabotropic glutamate receptors: structure, activation mechanism and pharmacology, Curr. Drug Targets CNS Neurol. Disord., 1 (2002) 297-317.
[4] C. Ghelardini, C. Menicacci, D. Cerretani, E. Bianchi, Spinal administration of mGluR5 antagonist prevents the onset of bortezomib induced neuropathic pain in rat, Neuropharmacol., 86 (2014) 294-300.
[5] M.C. Montana, L.F. Cavallone, K.K. Stubbert, A.D. Stefanescu, E.D. Kharasch, R.W.t. Gereau, The metabotropic glutamate receptor subtype 5 antagonist fenobam is analgesic and has improved in vivo selectivity compared with the prototypical antagonist 2-methyl-6-(phenylethynyl)-pyridine, J. Pharmacol. Exp. Ther., 330 (2009) 834-843.
[6] F. Caraci, G. Battaglia, M.A. Sortino, S. Spampinato, G. Molinaro, A. Copani, F. Nicoletti, V. Bruno, Metabotropic glutamate receptors in neurodegeneration/neuroprotection: still a hot topic?, Neurochem. Int., 61 (2012) 559-565.
[7] A. Vallano, V. Fernandez-Duenas, G. Garcia-Negredo, M.A. Quijada, C.P. Simon, M.L. Cuffi, L. Carbonell, S. Sanchez, J.M. Arnau, F. Ciruela, Targeting striatal metabotropic glutamate receptor type 5 in Parkinson's disease: bridging molecular studies and clinical trials, CNS Neurol. Disord. Drug Targets, 12 (2013) 1128-1142.
[8] D. Petrov, I. Pedros, M.L. de Lemos, M. Pallas, A.M. Canudas, A. Lazarowski, C. Beas-Zarate, C. Auladell, J. Folch, A. Camins, Mavoglurant as a treatment for Parkinson's disease, Expert Opin. Investig. Drugs, 23 (2014) 1165-1179.
[9] C. Finlay, S. Duty, Therapeutic potential of targeting glutamate receptors in Parkinson's disease, J. Neural. Transm., 121 (2014) 861-880.
[10] A.S. Pop, B. Gomez-Mancilla, G. Neri, R. Willemsen, F. Gasparini, Fragile X syndrome: a preclinical review on metabotropic glutamate receptor 5 (mGluR5) antagonists and drug development, Psychopharmacology (Berl.), 231 (2014) 1217-1226.
[11] S. Jacquemont, E. Berry-Kravis, R. Hagerman, F. von Raison, F. Gasparini, G. Apostol, M. Ufer, V. Des Portes, B. Gomez-Mancilla, The challenges of clinical trials in fragile X syndrome, Psychopharmacology (Berl.), 231 (2014) 1237-1250.
[12] J.A. Quiroz, P. Tamburri, D. Deptula, L. Banken, U. Beyer, M. Rabbia, N. Parkar, P. Fontoura, L. Santarelli, Efficacy and Safety of Basimglurant as Adjunctive Therapy for Major Depression: A Randomized Clinical Trial, JAMA Psychiatry, 73 (2016) 675-684.
[13] W.O. Rohof, A. Lei, D.P. Hirsch, L. Ny, M. Astrand, M.B. Hansen, G.E. Boeckxstaens, The effects of a novel metabotropic glutamate receptor 5 antagonist (AZD2066) on transient lower oesophageal sphincter relaxations and reflux episodes in healthy volunteers, Aliment. Pharmacol. Ther., 35 (2012) 1231-1242.
[14] R.H. Porter, P.J. Roberts, D.E. Jane, J.C. Watkins, (S)-homoquisqualate: a potent agonist at the glutamate metabotropic receptor, Br. J. Pharmacol., 106 (1992) 509-510.
[15] D.E. Jane, P.L. Jones, P.C. Pook, T.E. Salt, D.C. Sunter, J.C. Watkins, Stereospecific antagonism by (+)-alpha-methyl-4-carboxyphenylglycine (MCPG) of

(1S,3R)-ACPD-induced effects in neonatal rat motoneurones and rat thalamic neurones, Neuropharmacol., 32 (1993) 725-727.
[16] P. Wellendorph, H. Brauner-Osborne, Molecular basis for amino acid sensing by family C G-protein-coupled receptors, Br. J. Pharmacol., 156 (2009) 869-884.
[17] P.J. Flor, F.C. Acher, Orthosteric versus allosteric GPCR activation: the great challenge of group-III mGluRs, Biochem. Pharmacol., 84 (2012) 414-424.
[18] F. Kesisoglou, S. Panmai, Y. Wu, Nanosizing--oral formulation development and biopharmaceutical evaluation, Adv. Drug. Deliv. Rev., 59 (2007) 631-644.
[19] W.M. Pardridge, Drug transport across the blood-brain barrier, J. Cereb. Blood. Flow. Metab., 32 (2012) 1959-1972.
[20] T. de Paulis, K. Hemstapat, Y. Chen, Y. Zhang, S. Saleh, D. Alagille, R.M. Baldwin, G.D. Tamagnan, P.J. Conn, Substituent effects of N-(1,3-diphenyl-1H-pyrazol-5-yl)benzamides on positive allosteric modulation of the metabotropic glutamate-5 receptor in rat cortical astrocytes, J. Med. Chem., 49 (2006) 3332-3344.
[21] S. Conde-Ceide, C.M. Martinez-Viturro, J. Alcazar, P.M. Garcia-Barrantes, H. Lavreysen, C. Mackie, P.N. Vinson, J.M. Rook, T.M. Bridges, J.S. Daniels, A. Megens, X. Langlois, W.H. Drinkenburg, A. Ahnaou, C.M. Niswender, C.K. Jones, G.J. Macdonald, T. Steckler, P.J. Conn, S.R. Stauffer, J.M. Bartolome-Nebreda, C.W. Lindsley, Discovery of VU0409551/JNJ-46778212: An mGlu5 Positive Allosteric Modulator Clinical Candidate Targeting Schizophrenia, ACS Med. Chem. Lett., 6 (2015) 716-720.
[22] R.H. Porter, G. Jaeschke, W. Spooren, T.M. Ballard, B. Buttelmann, S. Kolczewski, J.U. Peters, E. Prinssen, J. Wichmann, E. Vieira, A. Muhlemann, S. Gatti, V. Mutel, P. Malherbe, Fenobam: a clinically validated nonbenzodiazepine anxiolytic is a potent, selective, and noncompetitive mGlu5 receptor antagonist with inverse agonist activity, J. Pharmacol. Exp. Ther., 315 (2005) 711-721.
[23] F. Gasparini, K. Lingenhohl, N. Stoehr, P.J. Flor, M. Heinrich, I. Vranesic, M. Biollaz, H. Allgeier, R. Heckendorn, S. Urwyler, M.A. Varney, E.C. Johnson, S.D. Hess, S.P. Rao, A.I. Sacaan, E.M. Santori, G. Velicelebi, R. Kuhn, 2-Methyl-6-(phenylethynyl)-pyridine (MPEP), a potent, selective and systemically active mGlu5 receptor antagonist, Neuropharmacol., 38 (1999) 1493-1503.
[24] C. Keywood, M. Wakefield, J. Tack, A proof-of-concept study evaluating the effect of ADX10059, a metabotropic glutamate receptor-5 negative allosteric modulator, on acid exposure and symptoms in gastro-oesophageal reflux disease, Gut, 58 (2009) 1192-1199.
[25] I. Vranesic, S. Ofner, P.J. Flor, G. Bilbe, R. Bouhelal, A. Enz, S. Desrayaud, K. McAllister, R. Kuhn, F. Gasparini, AFQ056/mavoglurant, a novel clinically effective mGluR5 antagonist: identification, SAR and pharmacological characterization, Bioorg. Med. Chem., 22 (2014) 5790-5803.
[26] A.S. Dore, K. Okrasa, J.C. Patel, M. Serrano-Vega, K. Bennett, R.M. Cooke, J.C. Errey, A. Jazayeri, S. Khan, B. Tehan, M. Weir, G.R. Wiggin, F.H. Marshall, Structure of class C GPCR metabotropic glutamate receptor 5 transmembrane domain, Nature, 511 (2014) 557-562.
[27] M.A. Varney, N.D. Cosford, C. Jachec, S.P. Rao, A. Sacaan, F.F. Lin, L. Bleicher, E.M. Santori, P.J. Flor, H. Allgeier, F. Gasparini, R. Kuhn, S.D. Hess, G. Velicelebi, E.C. Johnson, SIB-1757 and SIB-1893: selective, noncompetitive antagonists of metabotropic glutamate receptor type 5, J. Pharmacol. Exp. Ther., 290 (1999) 170-181.
[28] S. Pittolo, X. Gomez-Santacana, K. Eckelt, X. Rovira, J. Dalton, C. Goudet, J.P. Pin, A. Llobet, J. Giraldo, A. Llebaria, P. Gorostiza, An allosteric modulator to control endogenous G protein-coupled receptors with light, Nat. Chem. Biol., 10 (2014) 813-815.
[29] X. Gómez-Santacana, X. Rovira, J.A. Dalton, C. Goudet, J.P. Pin, P. Gorostiza, J. Giraldo, A. Llebaria, A double effect molecular switch leads to a novel potent negative allosteric modulator of metabotropic glutamate receptor 5, MedChemComm, 5 (2014) 1548-1554.

[30] B.H. Kaae, K. Harpsoe, T. Kvist, J.M. Mathiesen, C. Molck, D. Gloriam, H.N. Jimenez, M.A. Uberti, S.M. Nielsen, B. Nielsen, H. Brauner-Osborne, P. Sauerberg, R.P. Clausen, U. Madsen, Structure-activity relationships for negative allosteric mGluR5 modulators, ChemMedChem, 7 (2012) 440-451.
[31] K.A. Bennett, A.S. Dore, J.A. Christopher, D.R. Weiss, F.H. Marshall, Structures of mGluRs shed light on the challenges of drug development of allosteric modulators, Curr. Opin. Pharmacol., 20 (2015) 1-7.
[32] X. Rovira, A. Trapero, S. Pittolo, C. Zussy, A. Faucherre, C. Jopling, J. Giraldo, J.P. Pin, P. Gorostiza, C. Goudet, A. Llebaria, OptoGluNAM4.1, a Photoswitchable Allosteric Antagonist for Real-Time Control of mGlu4 Receptor Activity, Cell Chem. Biol., 23 (2016) 929-934.
[33] J.A. Dalton, I. Lans, X. Rovira, F. Malhaire, X. Gómez-Santacana, S. Pittolo, P. Gorostiza, A. Llebaria, C. Goudet, J.P. Pin, J. Giraldo, Shining Light On An mGlu5 Photoswitchable NAM: A Theoretical Perspective, Curr. Neuropharmacol., 14 (2016) 441-454.
[34] S. Samanta, H.I. Qureshi, G.A. Woolley, A bisazobenzene crosslinker that isomerizes with visible light, Beilstein J. Org. Chem., 8 (2012) 2184-2190.
[35] C. Molck, K. Harpsoe, D.E. Gloriam, R.P. Clausen, U. Madsen, L.O. Pedersen, H.N. Jimenez, S.M. Nielsen, J.M. Mathiesen, H. Brauner-Osborne, Pharmacological characterization and modeling of the binding sites of novel 1,3-bis(pyridinylethynyl)benzenes as metabotropic glutamate receptor 5-selective negative allosteric modulators, Mol. Pharmacol., 82 (2012) 929-937.
[36] X. Gómez-Santacana, S. Pittolo, X. Rovira, M. Lopez, C. Zussy, J.A.R. Dalton, A. Faucherre, C. Jopling, J.-P. Pin, F. Ciruela, C. Goudet, J. Giraldo, P. Gorostiza, A. Llebaria, Illuminating Phenylazopyridines To Photoswitch Metabotropic Glutamate Receptors: From the Flask to the Animals, ACS Cent. Sci., in press (2016) DOI: 10.1021/acscentsci.1026b00353.
[37] J.A. Christopher, S.J. Aves, K.A. Bennett, A.S. Dore, J.C. Errey, A. Jazayeri, F.H. Marshall, K. Okrasa, M.J. Serrano-Vega, B.G. Tehan, G.R. Wiggin, M. Congreve, Fragment and Structure-Based Drug Discovery for a Class C GPCR: Discovery of the mGlu5 Negative Allosteric Modulator HTL14242 (3-Chloro-5-[6-(5-fluoropyridin-2-yl)pyrimidin-4-yl]benzonitrile), J. Med. Chem., 58 (2015) 6653-6664.
[38] H. Wu, C. Wang, K.J. Gregory, G.W. Han, H.P. Cho, Y. Xia, C.M. Niswender, V. Katritch, J. Meiler, V. Cherezov, P.J. Conn, R.C. Stevens, Structure of a class C GPCR metabotropic glutamate receptor 1 bound to an allosteric modulator, Science, 344 (2014) 58-64.
[39] J. Broichhagen, J.A. Frank, D. Trauner, A roadmap to success in photopharmacology, Acc. Chem. Res., 48 (2015) 1947-1960.
[40] R.W. Gould, R.J. Amato, M. Bubser, M.E. Joffe, M.T. Nedelcovych, A.D. Thompson, H.H. Nickols, J.P. Yuh, X. Zhan, A.S. Felts, A.L. Rodriguez, R.D. Morrison, F.W. Byers, J.M. Rook, J.S. Daniels, C.M. Niswender, P.J. Conn, K.A. Emmitte, C.W. Lindsley, C.K. Jones, Partial mGlu Negative Allosteric Modulators Attenuate Cocaine-Mediated Behaviors and Lack Psychotomimetic-Like Effects, Neuropsychopharmacology, (2015).
[41] H.H. Nickols, J.P. Yuh, K.J. Gregory, R.D. Morrison, B.S. Bates, S.R. Stauffer, K.A. Emmitte, M. Bubser, W. Peng, M.T. Nedelcovych, A. Thompson, X. Lv, Z. Xiang, J.S. Daniels, C.M. Niswender, C.W. Lindsley, C.K. Jones, P.J. Conn, VU0477573: Partial negative allosteric modulator of the subtype 5 metabotropic glutamate receptor with in vivo efficacy, J. Pharmacol. Exp. Ther., (2015).
[42] K. Abou Farha, R. Bruggeman, C. Balje-Volkers, Metabotropic glutamate receptor 5 negative modulation in phase I clinical trial: potential impact of circadian rhythm on the neuropsychiatric adverse reactions-do hallucinations matter?, ISRN Psychiatry, 2014 (2014) 652750.

[43] U.C. Campbell, K. Lalwani, L. Hernandez, G.G. Kinney, P.J. Conn, L.J. Bristow, The mGluR5 antagonist 2-methyl-6-(phenylethynyl)-pyridine (MPEP) potentiates PCP-induced cognitive deficits in rats, Psychopharmacology (Berl.), 175 (2004) 310-318.
[44] I. Brabet, M.L. Parmentier, C. De Colle, J. Bockaert, F. Acher, J.P. Pin, Comparative effect of L-CCG-I, DCG-IV and gamma-carboxy-L-glutamate on all cloned metabotropic glutamate receptor subtypes, Neuropharmacol., 37 (1998) 1043-1051.
[45] G.M. Morris, R. Huey, W. Lindstrom, M.F. Sanner, R.K. Belew, D.S. Goodsell, A.J. Olson, AutoDock4 and AutoDockTools4: Automated docking with selective receptor flexibility, J. Comput. Chem., 30 (2009) 2785-2791.
[46] D.A. Case, T.E. Cheatham, 3rd, T. Darden, H. Gohlke, R. Luo, K.M. Merz, Jr., A. Onufriev, C. Simmerling, B. Wang, R.J. Woods, The Amber biomolecular simulation programs, J. Comput. Chem., 26 (2005) 1668-1688.
[47] E.F. Pettersen, T.D. Goddard, C.C. Huang, G.S. Couch, D.M. Greenblatt, E.C. Meng, T.E. Ferrin, UCSF Chimera--a visualization system for exploratory research and analysis, J. Comput. Chem., 25 (2004) 1605-1612.

ACCEPTED MANUSCRIPT

ACCEPTED MANUSCRIPT

Highlights

- Efficacy of bispyridine benzene mGlu5 negative allosteric modulators depends on molecule geometry.
- 1,4-disubstituted linear compounds have $mGlu_5$ partial antagonist activity.
- 1,3-disubstituted angular compounds have $mGlu_5$ full inverse agonist activity.
- 1,4- and 1,3-isomers bind preferentially to different receptor conformations according to computational docking.

ACCEPTED MANUSCRIPT

ACCEPTED MANUSCRIPT

Supplementary Material

Positional isomers of bispyridine benzene derivatives induce efficacy changes on $mGlu_5$ negative allosteric modulation

Xavier Gómez-Santacana[a,b,c,§], James A. R. Dalton[b,d], Xavier Rovira [e,f], Jean Philippe Pin [e,f], Cyril Goudet [e,f], Pau Gorostiza[c,g,h], Jesús Giraldo[b,d] and Amadeu Llebaria[a*]

(a) MCS, Laboratory of Medicinal Chemistry & Synthesis, Institute for Advanced Chemistry of Catalonia (IQAC−CSIC), Jordi Girona 18-26, 08034 Barcelona, Spain.

(b) Laboratory of Molecular Neuropharmacology and Bioinformatics, Institut de Neurociències and Unitat de Bioestadística, Universitat Autònoma de Barcelona (UAB), 08193 Bellaterra, Spain.

(c) Nanoprobes and Nanoswitches, Institute for Bioengineering of Catalonia (IBEC), Baldiri Reixac, 08028, Barcelona, Spain.

(d) Network Biomedical Research Center on Mental Health (CIBERSAM), Spain

(e) Department of Neurosciences, Institute of Functional Genomics, Université de Montpellier, Unité Mixte de Recherche 5302 CNRS, Montpellier, France; (f) Unité de recherche U1191, INSERM, Montpellier, France (g) Network Biomedical Research Center on Bioengineering, Biomaterials and Nanomedicine (CIBER-BBN), Spain.

(h) Catalan Institution for Research and Advanced Studies (ICREA), Barcelona, Spain.

(§) Present address: Division of Medicinal Chemistry, Amsterdam Institute for Molecules, Medicines and Systems (AIMMS), VU University Amsterdam, The Netherlands.

* Corresponding author: amadeu.llebaria@iqac.csic.es

1) Nuclear Magnetic Resonance Spectra
2) High Performance Liquid Chromatography coupled to a Photodiode Array and Mass Spectrometer
3) UV/Vis spectra under illumination

ACCEPTED MANUSCRIPT

ACCEPTED MANUSCRIPT

1) Nuclear Magnetic Resonance Spectra

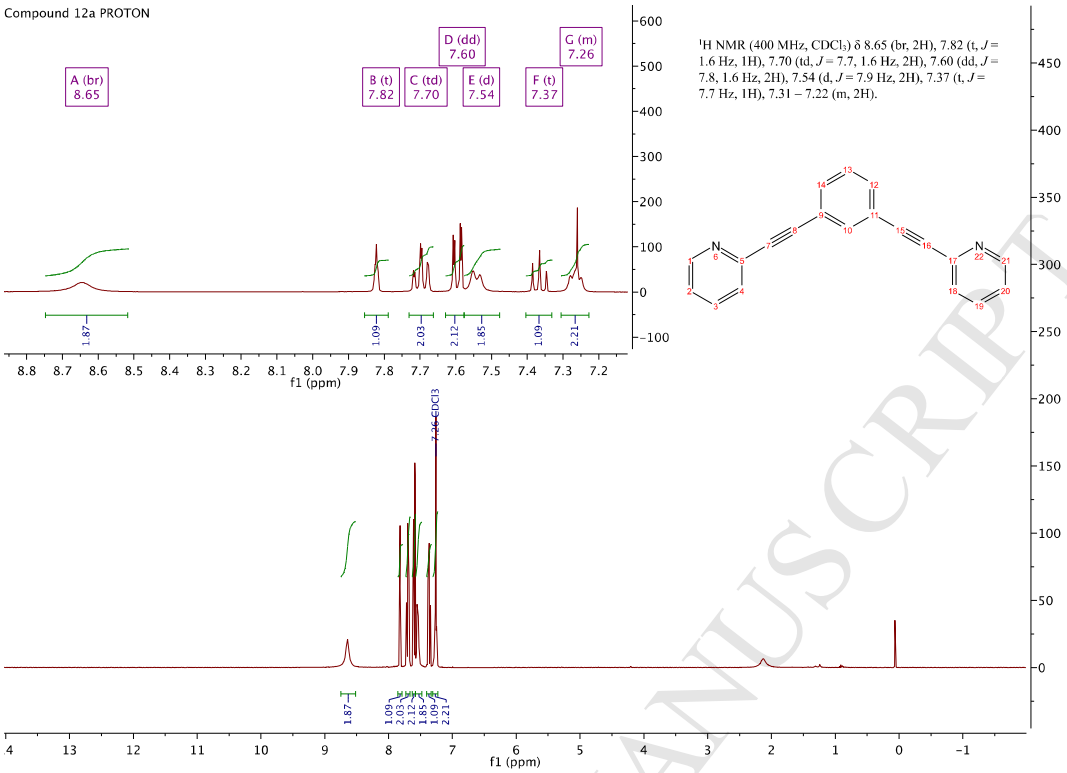

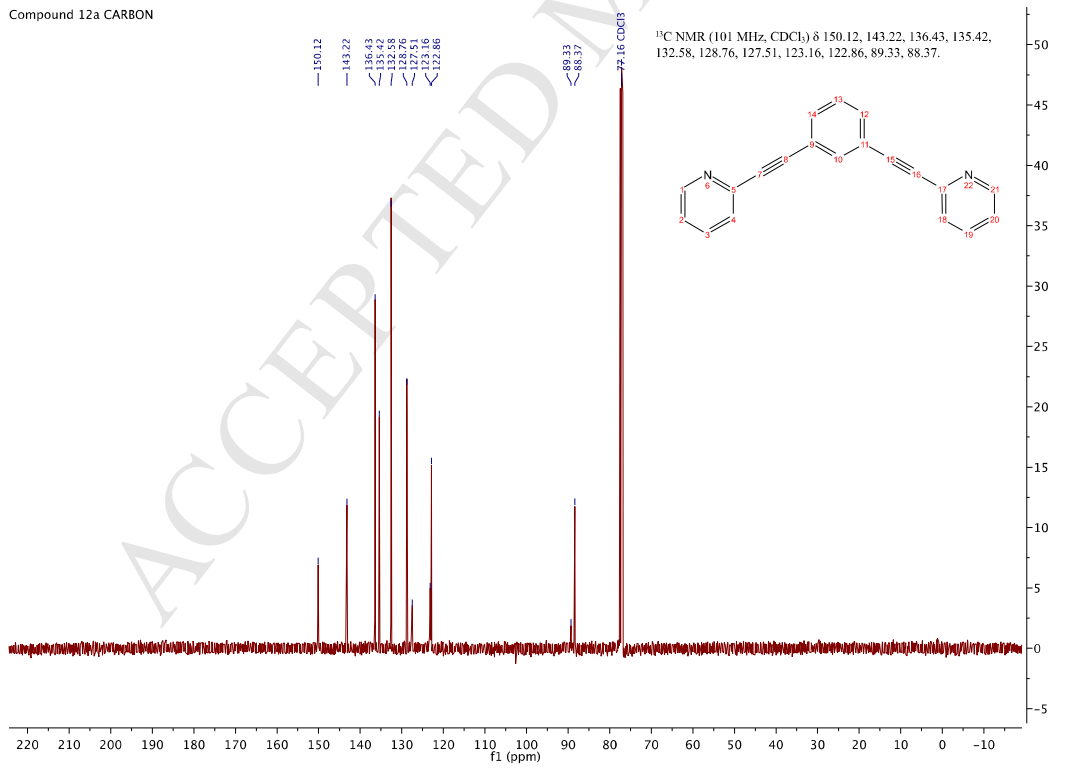

Compound 12b PROTON

^{1}H NMR (400 MHz, $CDCl_3$) δ 8.65 (br, 2H), 7.72 (td, J = 7.7, 1.6 Hz, 2H), 7.60 (s, 4H), 7.56 (d, J = 8.0 Hz, 2H), 7.28 (dd, J = 6.9, 5.3 Hz, 2H).

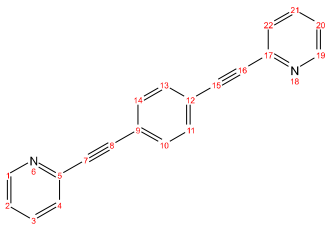

Compound 17a PROTON

^{1}H NMR (400 MHz, $CDCl_3$) δ 8.61 (ddd, J = 4.9, 1.8, 1.0 Hz, 1H), 7.67 (td, J = 7.7, 1.8 Hz, 1H), 7.50 (dt, J = 7.9, 1.1 Hz, 1H), 7.23 (ddd, J = 7.6, 4.9, 1.2 Hz, 1H), 7.14 (t, J = 7.8 Hz, 1H), 7.00 (dt, J = 7.6, 1.2 Hz, 1H), 6.91 (dd, J = 2.4, 1.5 Hz, 1H), 6.69 (ddd, J = 8.1, 2.4, 1.0 Hz, 1H), 3.13 (br, 2H).

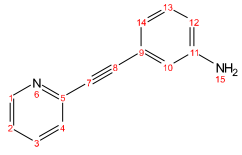

Compound 17a CARBON

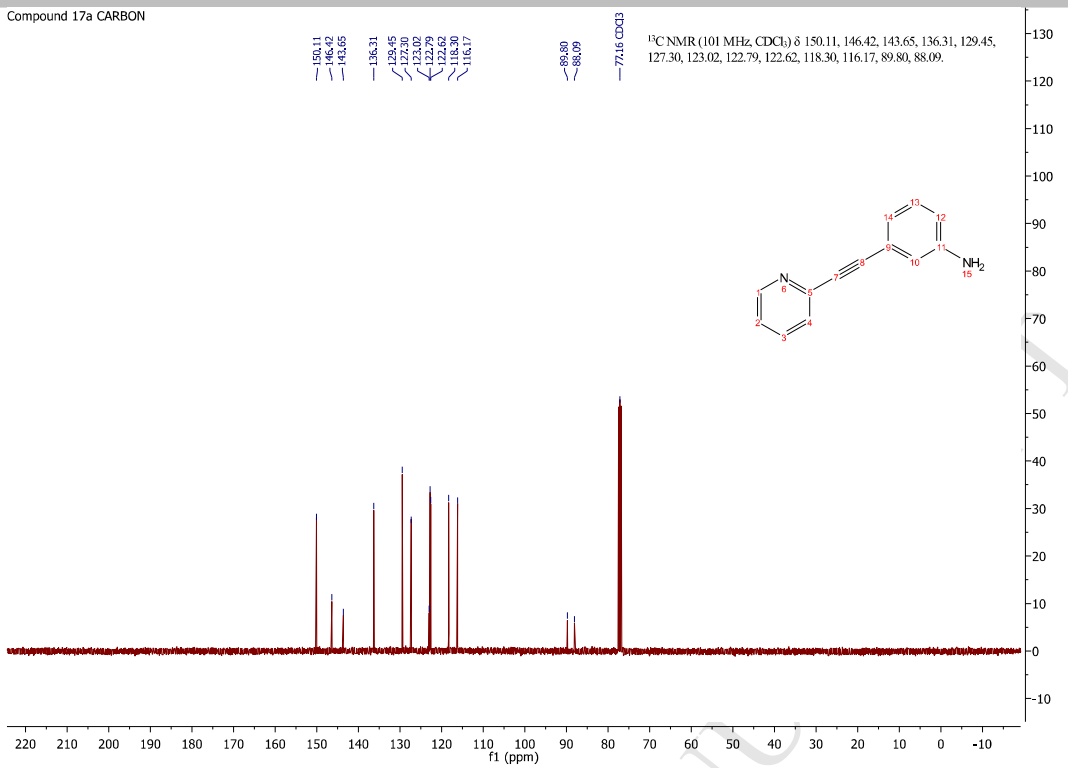

^{13}C NMR (101 MHz, $CDCl_3$) δ 150.11, 146.42, 143.65, 136.31, 129.45, 127.30, 123.02, 122.79, 122.62, 118.30, 116.17, 89.80, 88.09.

Compound 17b PROTON

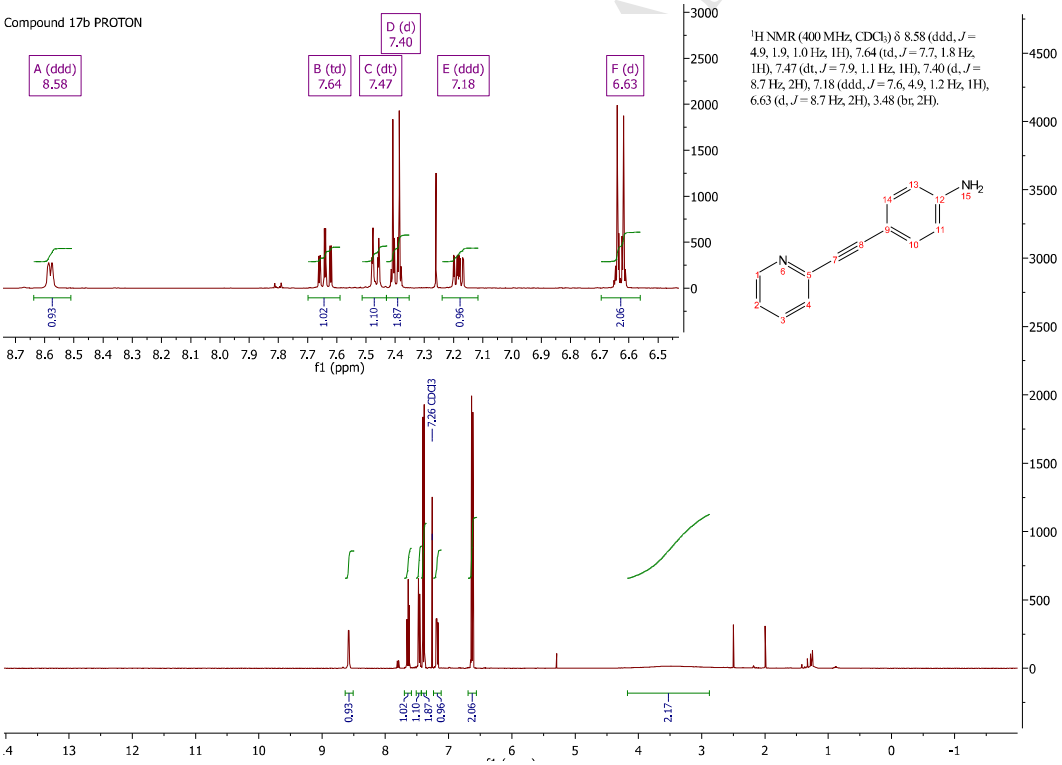

^{1}H NMR (400 MHz, $CDCl_3$) δ 8.58 (ddd, *J* = 4.9, 1.9, 1.0 Hz, 1H), 7.64 (td, *J* = 7.7, 1.8 Hz, 1H), 7.47 (dt, *J* = 7.9, 1.1 Hz, 1H), 7.40 (d, *J* = 8.7 Hz, 2H), 7.18 (ddd, *J* = 7.6, 4.9, 1.2 Hz, 1H), 6.63 (d, *J* = 8.7 Hz, 2H), 3.48 (br, 2H).

Compound 17b CARBON

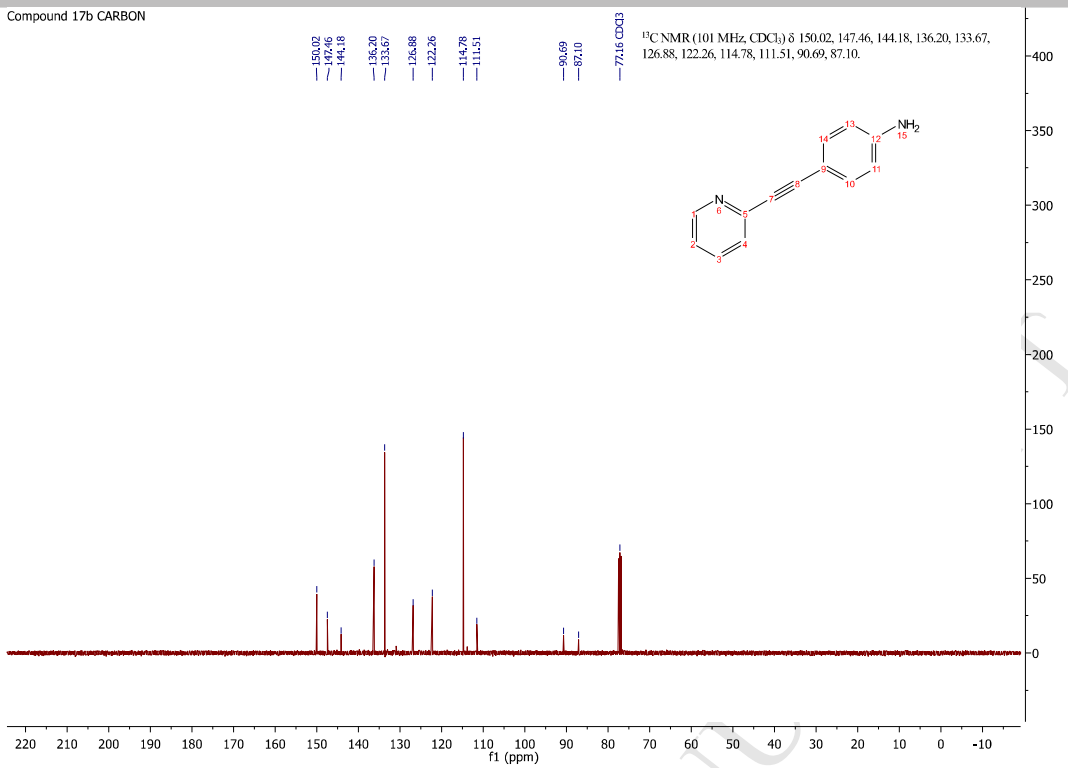

^{13}C NMR (101 MHz, $CDCl_3$) δ 150.02, 147.46, 144.18, 136.20, 133.67, 126.88, 122.26, 114.78, 111.51, 90.69, 87.10.

Compound 19a PROTON

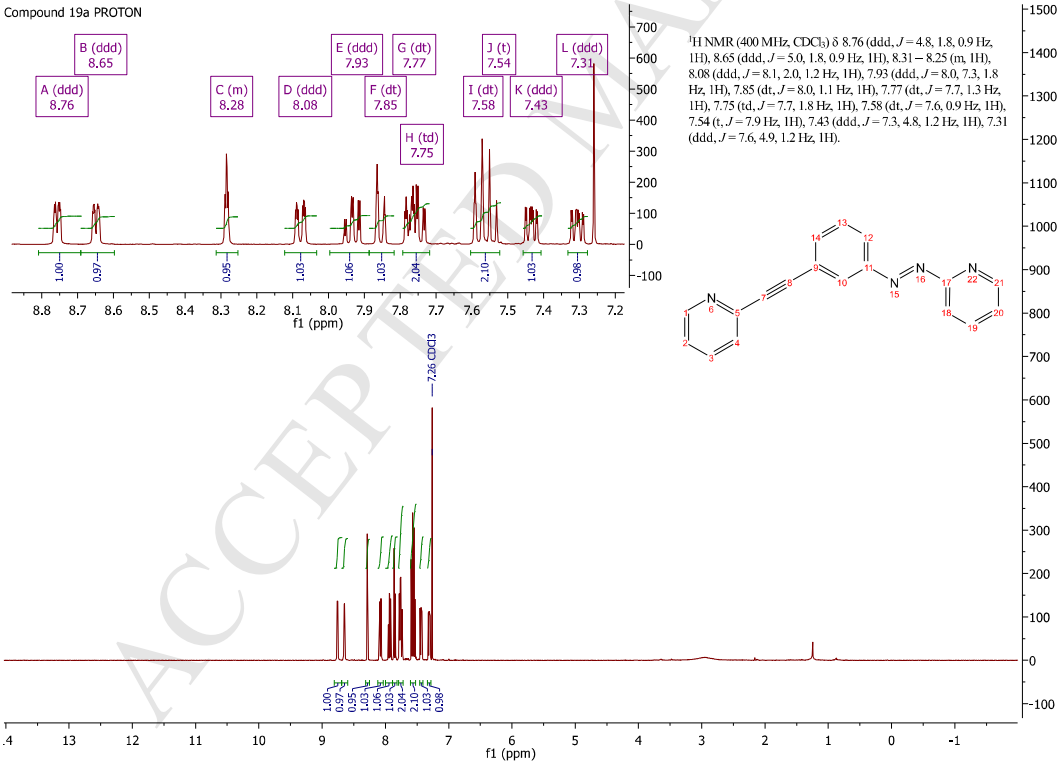

^{1}H NMR (400 MHz, $CDCl_3$) δ 8.76 (ddd, J = 4.8, 1.8, 0.9 Hz, 1H), 8.65 (ddd, J = 5.0, 1.8, 0.9 Hz, 1H), 8.31 – 8.25 (m, 1H), 8.08 (ddd, J = 8.1, 2.0, 1.2 Hz, 1H), 7.93 (ddd, J = 8.0, 7.3, 1.8 Hz, 1H), 7.85 (dt, J = 8.0, 1.1 Hz, 1H), 7.77 (dt, J = 7.7, 1.3 Hz, 1H), 7.75 (td, J = 7.7, 1.8 Hz, 1H), 7.58 (dt, J = 7.6, 0.9 Hz, 1H), 7.54 (t, J = 7.9 Hz, 1H), 7.43 (ddd, J = 7.3, 4.8, 1.2 Hz, 1H), 7.31 (ddd, J = 7.6, 4.9, 1.2 Hz, 1H).

ACCEPTED MANUSCRIPT

ACCEPTED MANUSCRIPT

Compound 19a CARBON

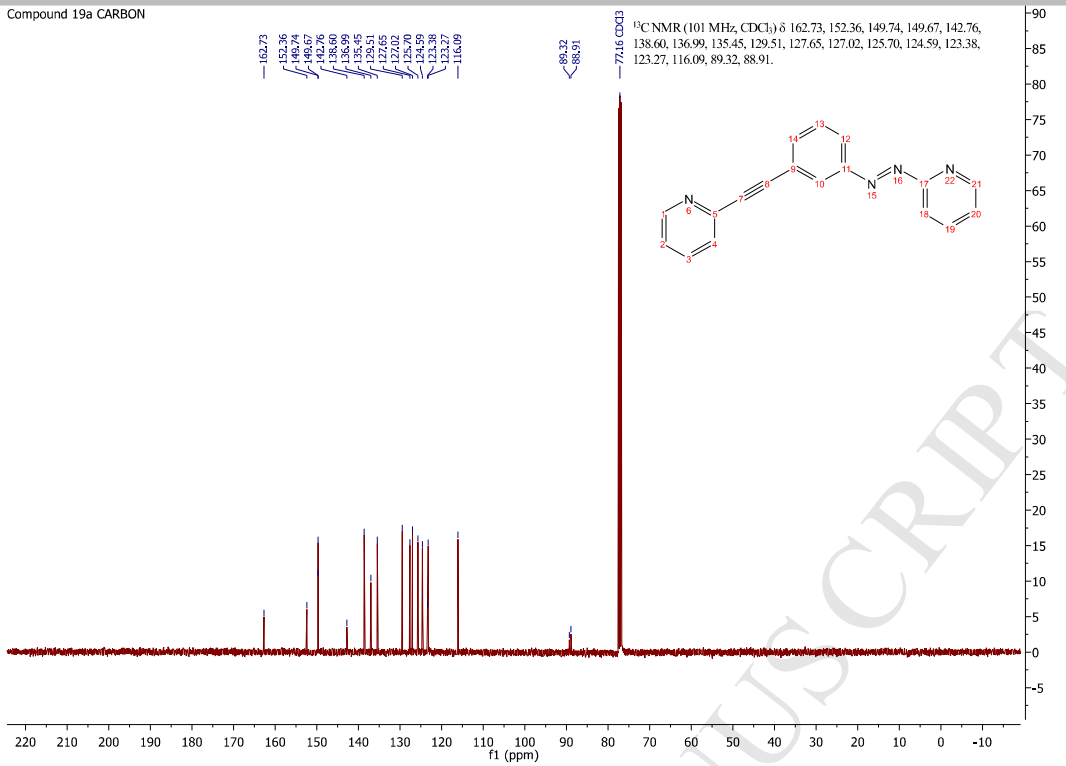

^{13}C NMR (101 MHz, $CDCl_3$) δ 162.73, 152.36, 149.74, 149.67, 142.76, 138.60, 136.99, 135.45, 129.51, 127.65, 127.02, 125.70, 124.59, 123.38, 123.27, 116.09, 89.32, 88.91.

Compound 19b PROTON

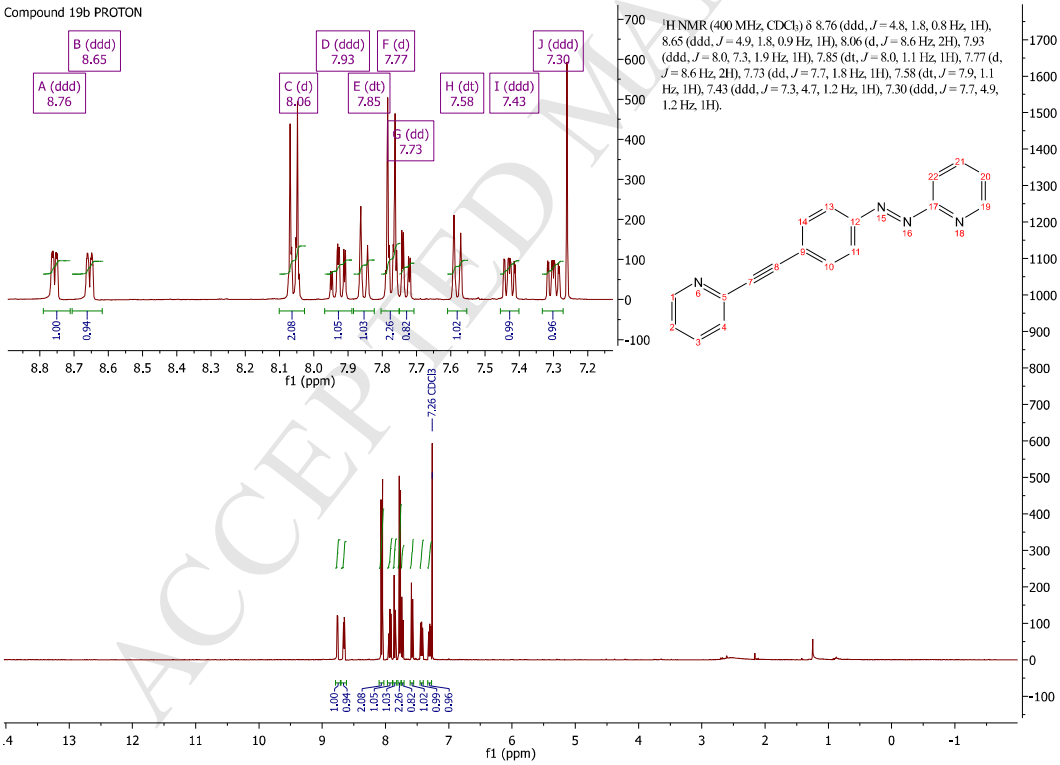

^{1}H NMR (400 MHz, $CDCl_3$) δ 8.76 (ddd, J = 4.8, 1.8, 0.8 Hz, 1H), 8.65 (ddd, J = 4.9, 1.8, 0.9 Hz, 1H), 8.06 (d, J = 8.6 Hz, 2H), 7.93 (ddd, J = 8.0, 7.3, 1.9 Hz, 1H), 7.85 (dt, J = 8.0, 1.1 Hz, 1H), 7.77 (d, J = 8.6 Hz, 2H), 7.73 (dd, J = 7.7, 1.8 Hz, 1H), 7.58 (dt, J = 7.9, 1.1 Hz, 1H), 7.43 (ddd, J = 7.3, 4.7, 1.2 Hz, 1H), 7.30 (ddd, J = 7.7, 4.9, 1.2 Hz, 1H).

ACCEPTED MANUSCRIPT

Compound 19b CARBON

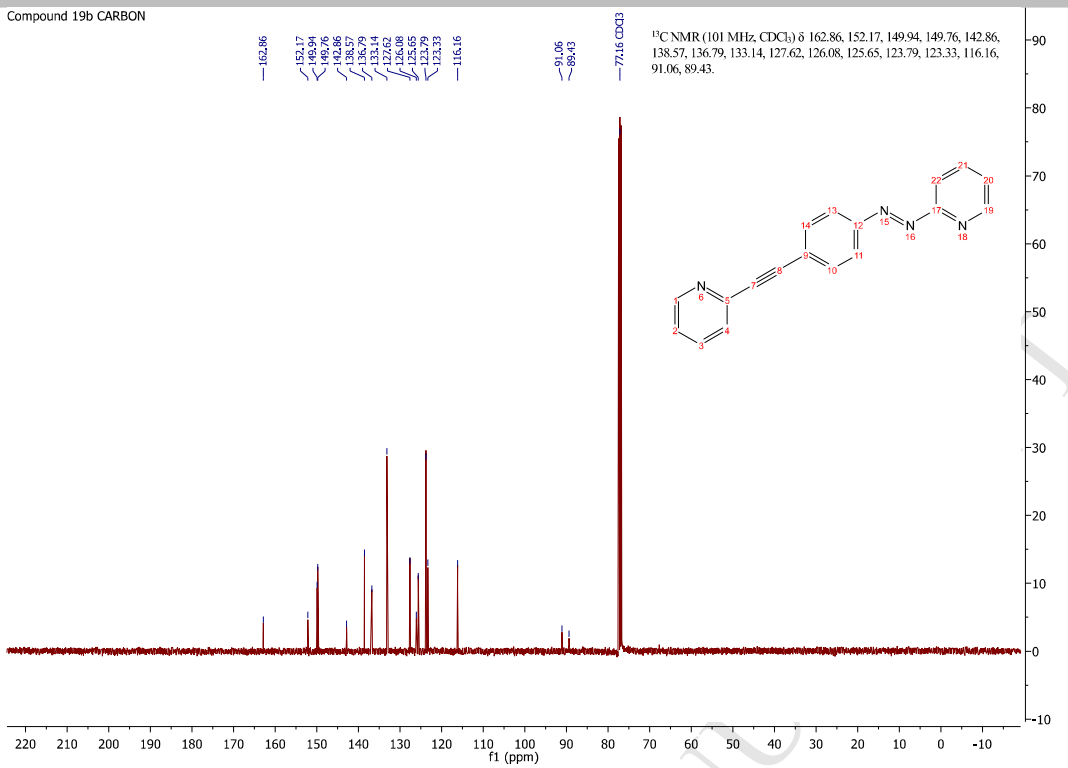

^{13}C NMR (101 MHz, $CDCl_3$) δ 162.86, 152.17, 149.94, 149.76, 142.86, 138.57, 136.79, 133.14, 127.62, 126.08, 125.65, 123.79, 123.33, 116.16, 91.06, 89.43.

Compound 21a PROTON

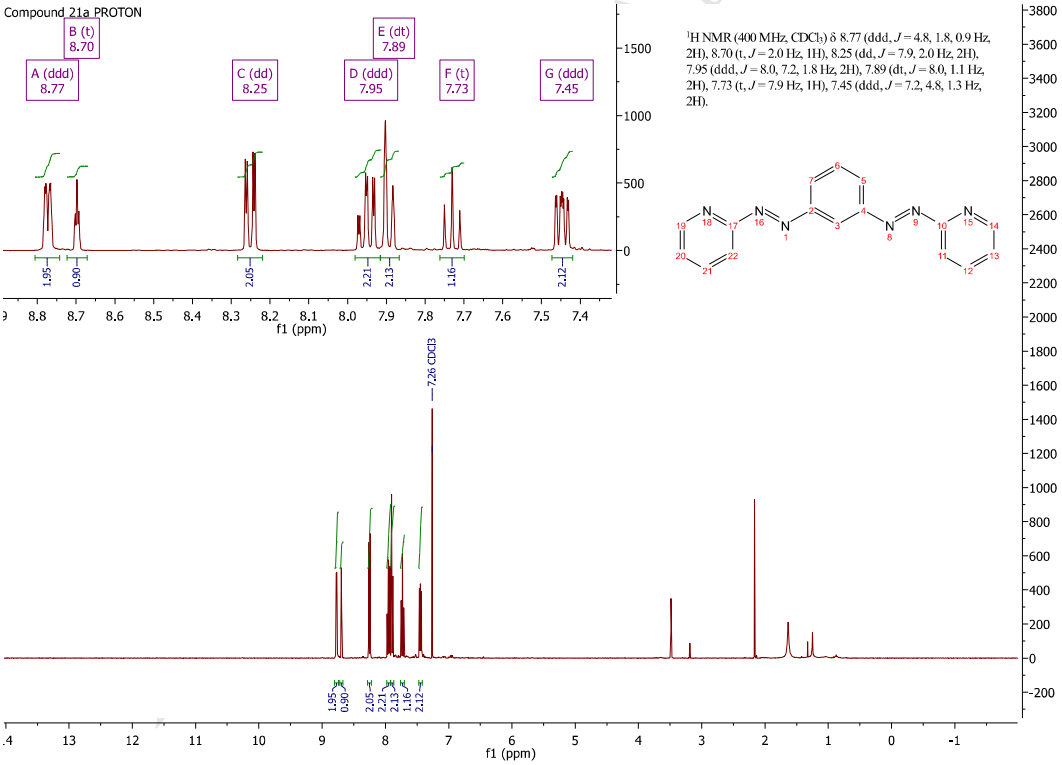

^{1}H NMR (400 MHz, $CDCl_3$) δ 8.77 (ddd, J = 4.8, 1.8, 0.9 Hz, 2H), 8.70 (t, J = 2.0 Hz, 1H), 8.25 (dd, J = 7.9, 2.0 Hz, 2H), 7.95 (ddd, J = 8.0, 7.2, 1.8 Hz, 2H), 7.89 (dt, J = 8.0, 1.1 Hz, 2H), 7.73 (t, J = 7.9 Hz, 1H), 7.45 (ddd, J = 7.2, 4.8, 1.3 Hz, 2H).

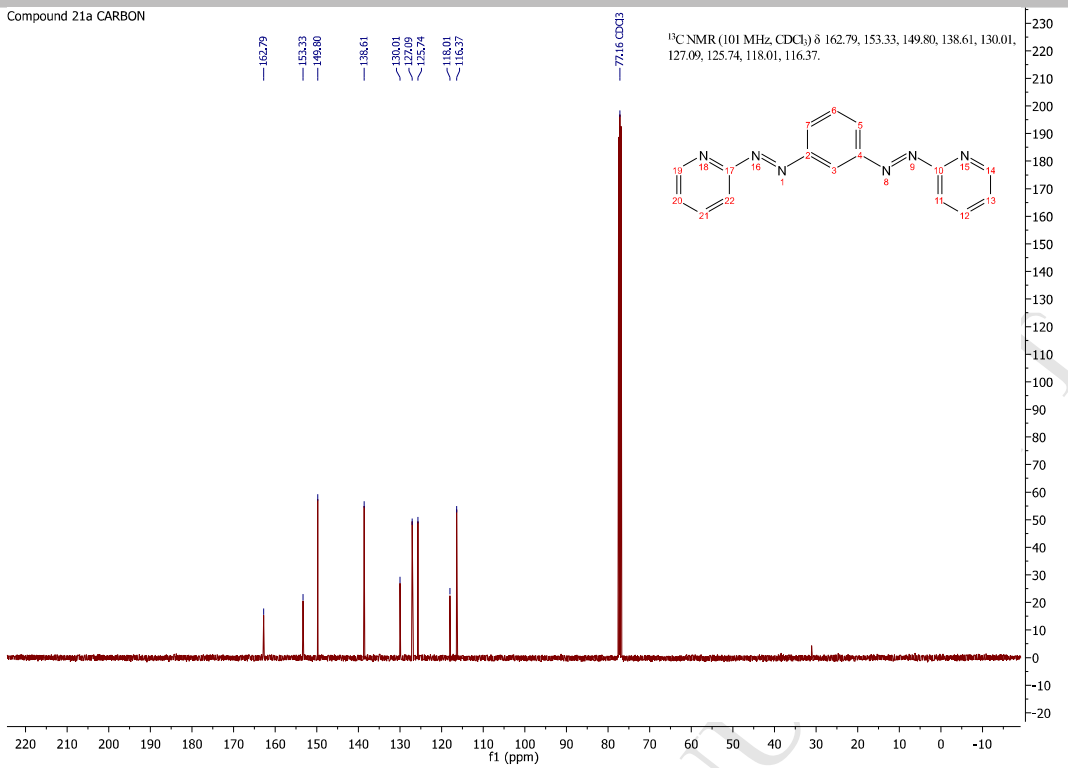
Compound 21a CARBON
162.79
153.33
149.80
138.61
130.01
127.09
125.74
118.01
116.37
77.16 CDCl3
^{13}C NMR (101 MHz, CDCl$_3$) δ 162.79, 153.33, 149.80, 138.61, 130.01, 127.09, 125.74, 118.01, 116.37.
f1 (ppm)

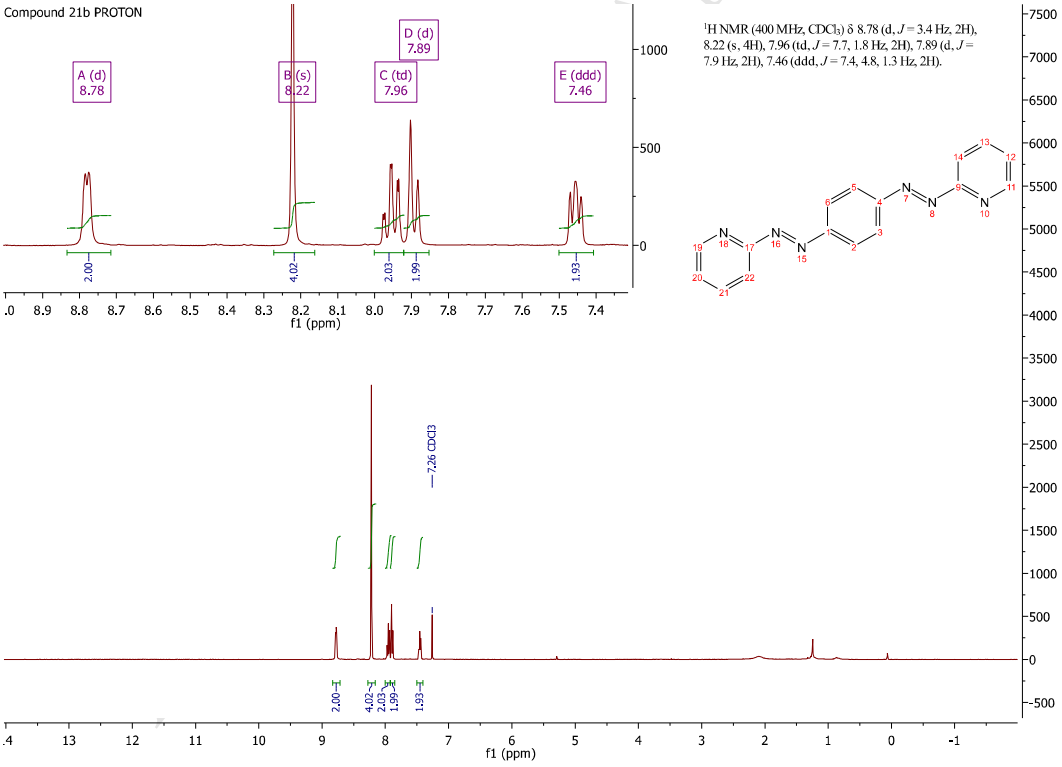
Compound 21b PROTON
A (d) 8.78
B (s) 8.22
C (td) 7.96
D (d) 7.89
E (ddd) 7.46
2.00
4.02
2.03
1.99
1.93
^{1}H NMR (400 MHz, CDCl$_3$) δ 8.78 (d, J = 3.4 Hz, 2H), 8.22 (s, 4H), 7.96 (td, J = 7.7, 1.8 Hz, 2H), 7.89 (d, J = 7.9 Hz, 2H), 7.46 (ddd, J = 7.4, 4.8, 1.3 Hz, 2H).
7.26 CDCl3
f1 (ppm)

ACCEPTED MANUSCRIPT

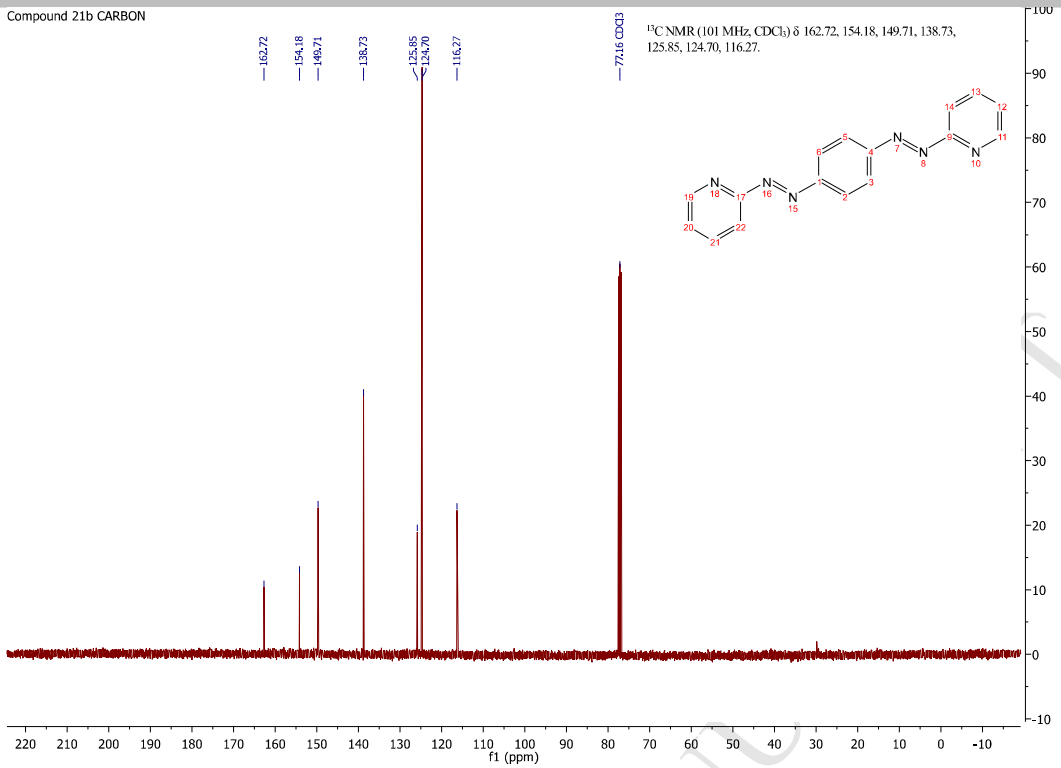

2) High Performance Liquid Chromatography coupled to a Photodiode Array and Mass Spectrometer

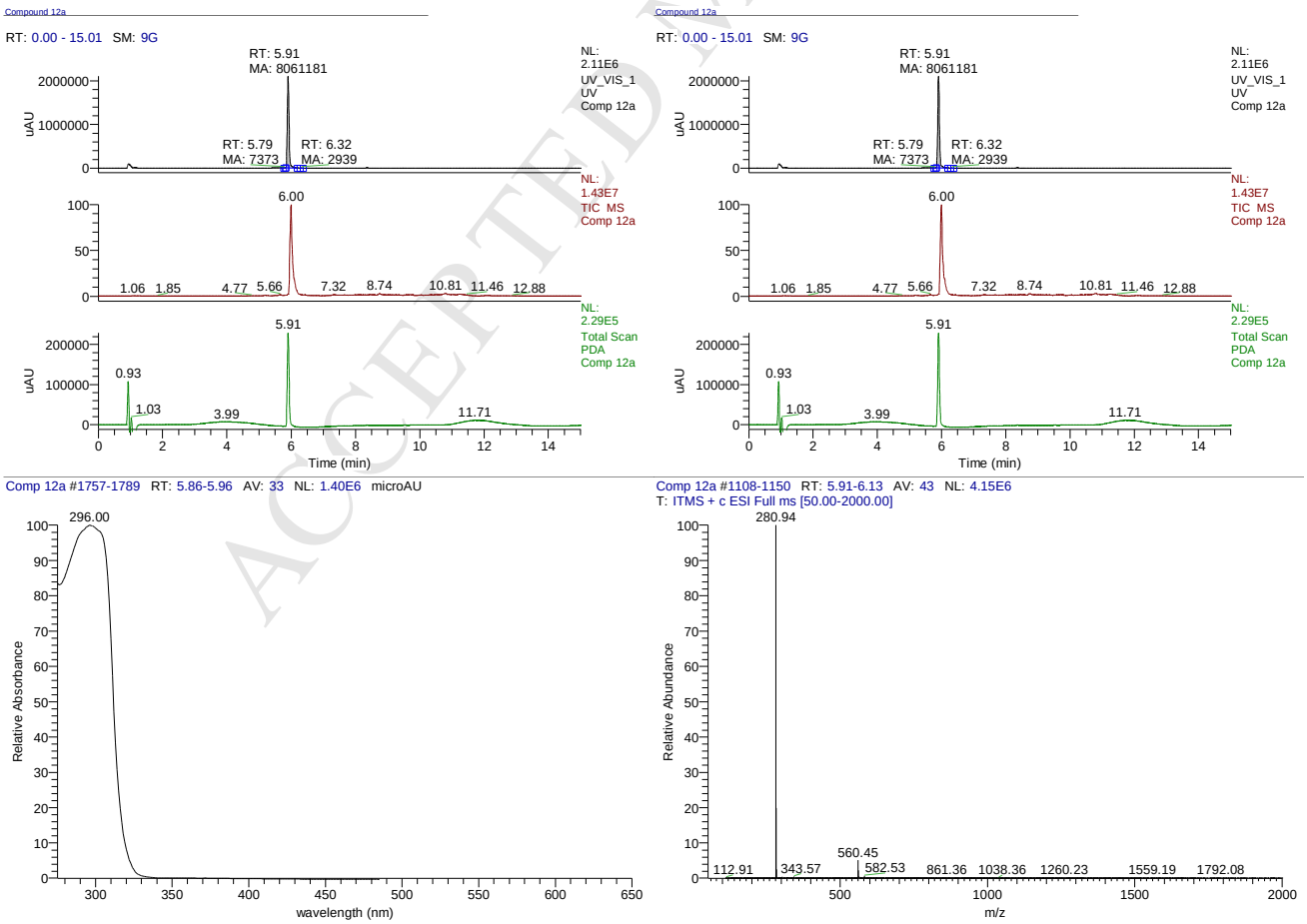

ACCEPTED MANUSCRIPT

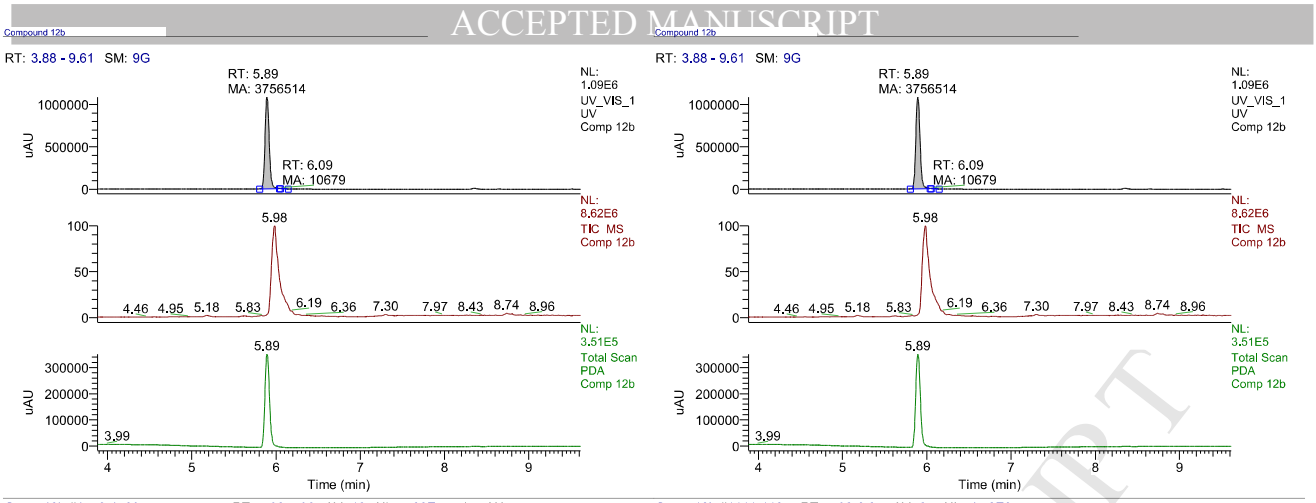

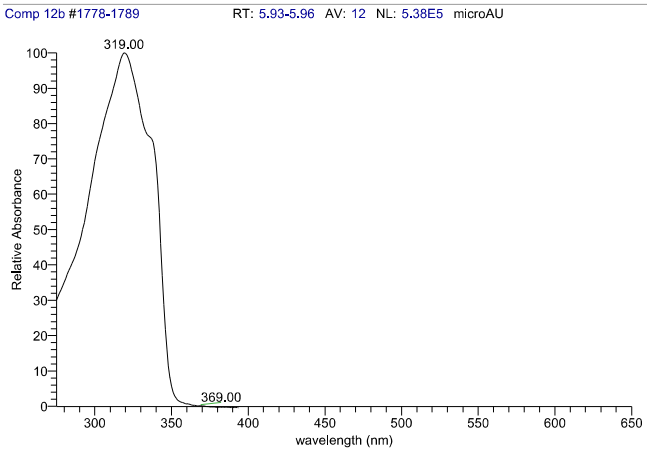

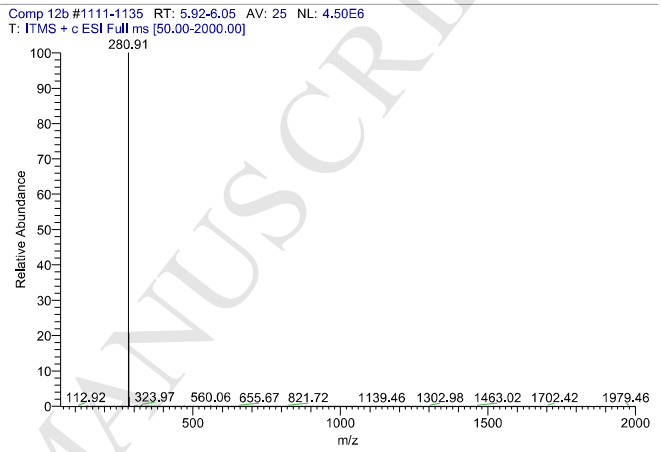

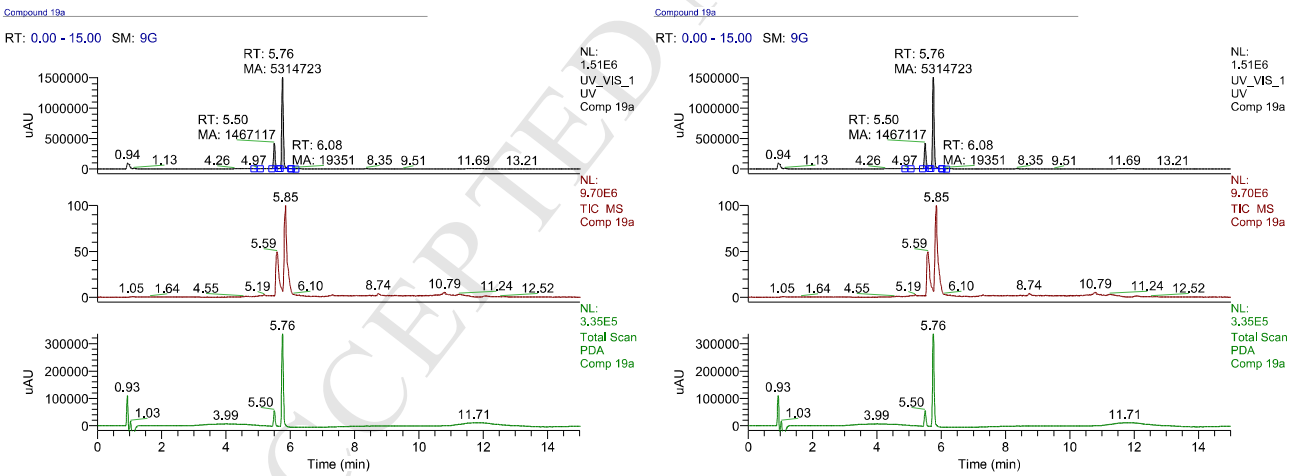

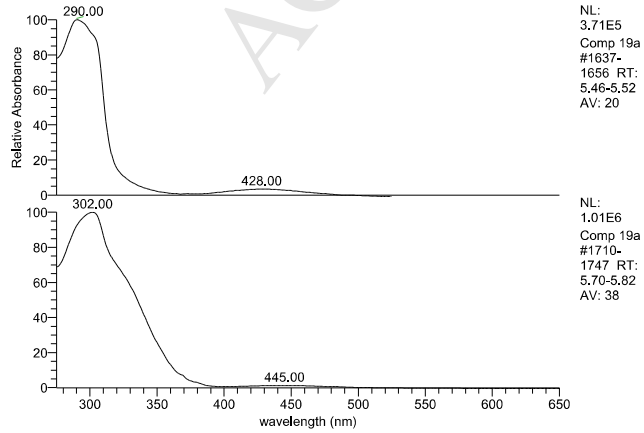

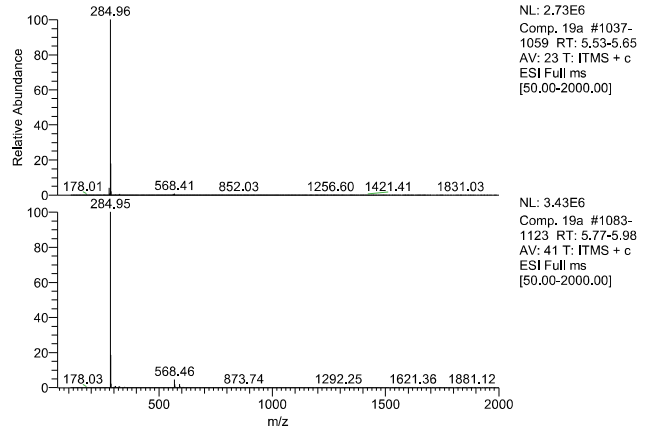

ACCEPTED MANUSCRIPT

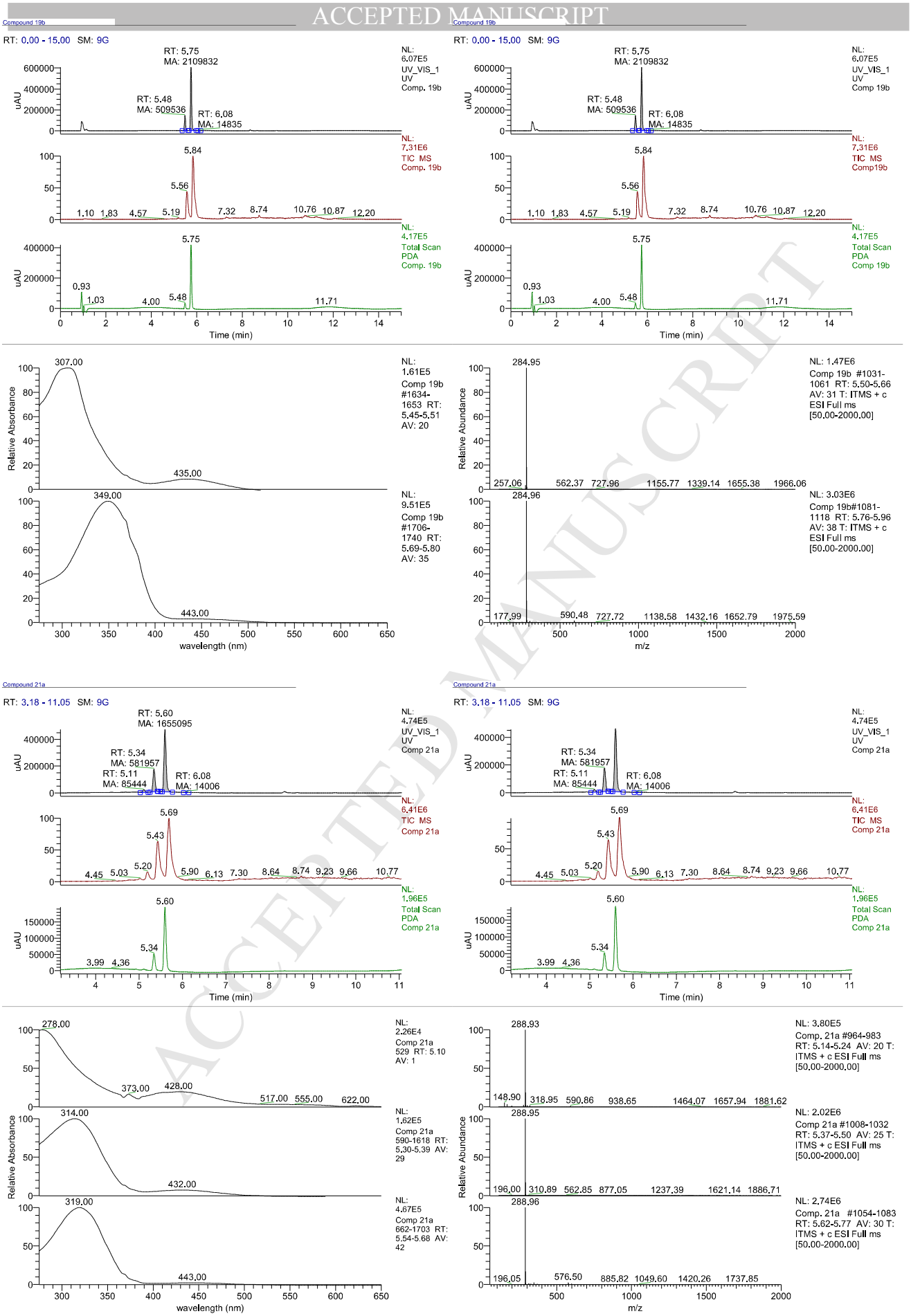

ACCEPTED MANUSCRIPT

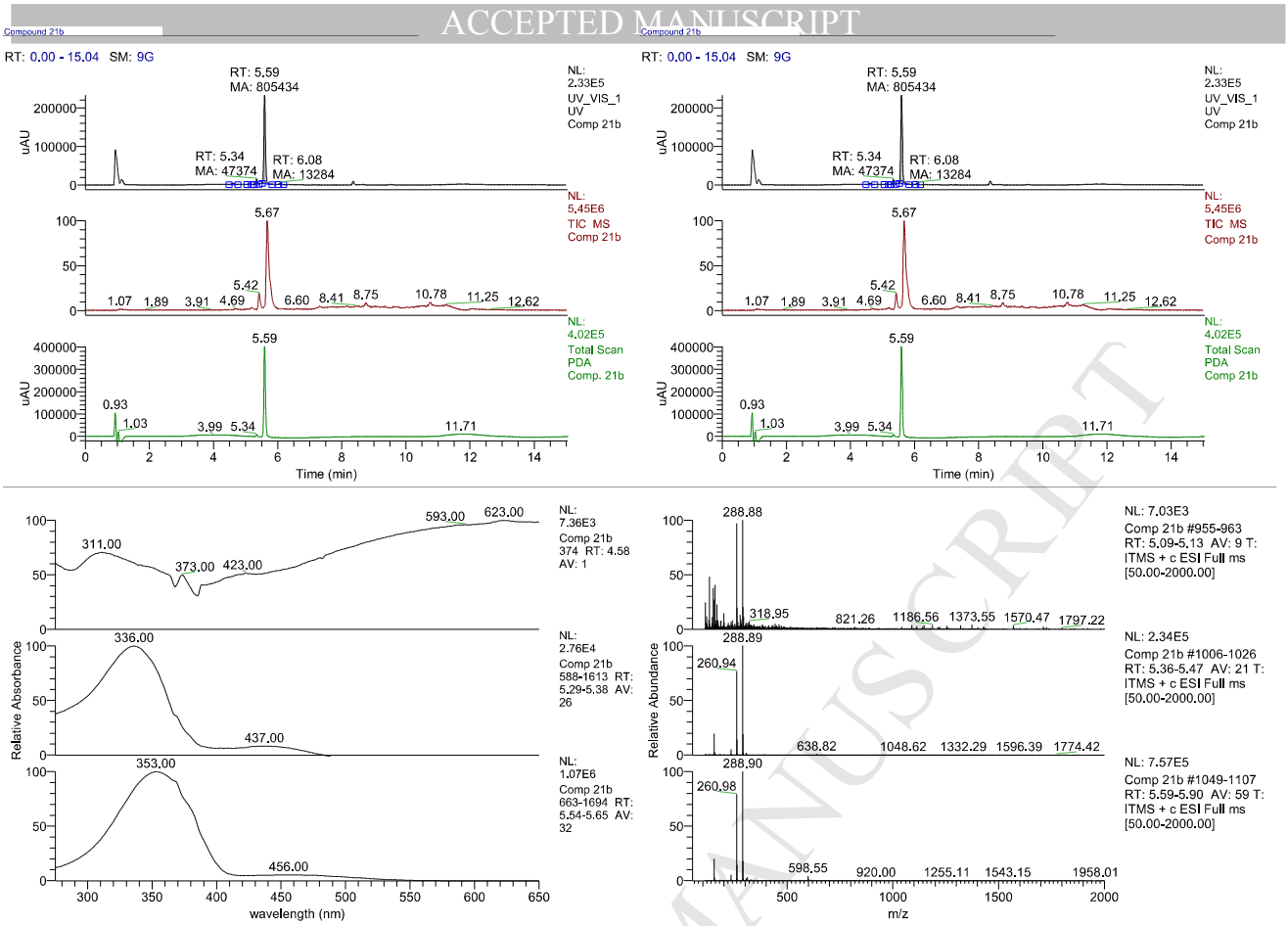

3) UV/Vis spectra under illumination

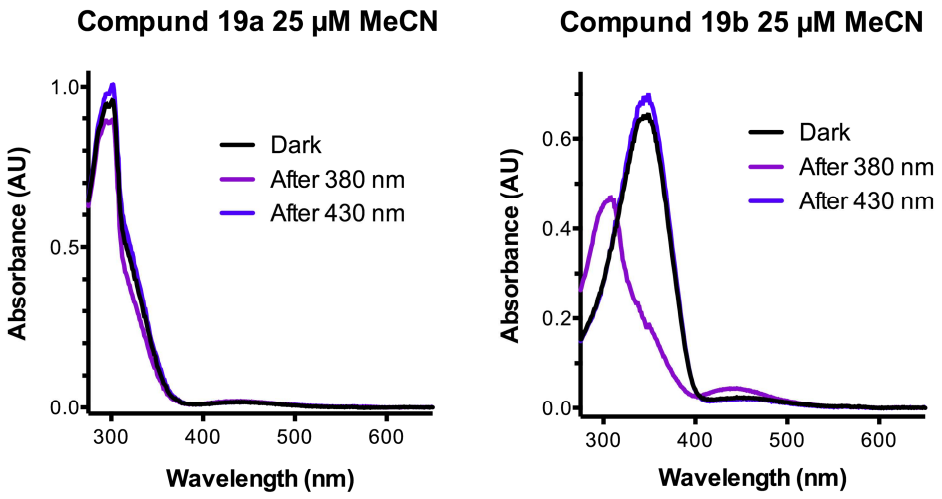

ACCEPTED MANUSCRIPT

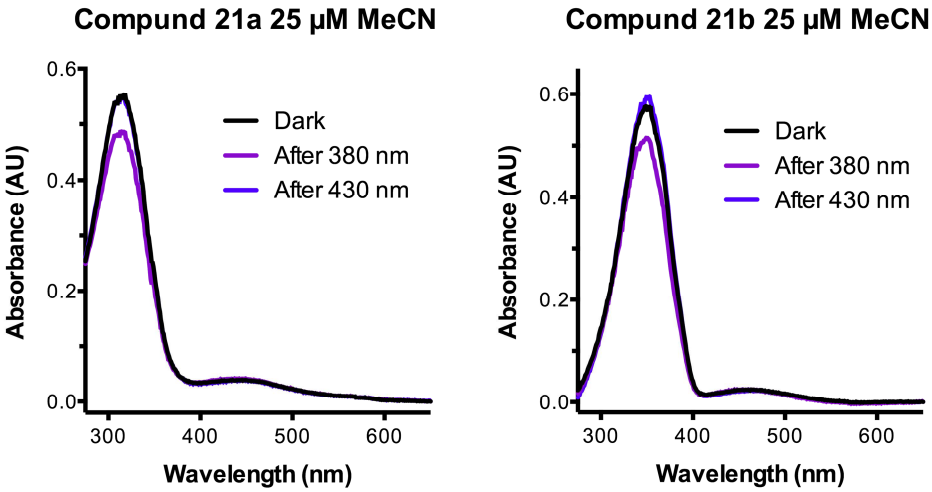

ACCEPTED MANUSCRIPT